Available online at www.sciencedirect.com
ScienceDirect
Trans. Nonferrous Met. Soc. China 34(2024) 3093−3117
Transactions of Nonferrous Metals Society of China
www.tnmsc.cn

Phase transformation in titanium alloys: A review

Chang-chang LIU, Yang-huan-zi LI, Ji GU, Min SONG

State Key Laboratory of Powder Metallurgy, Central South University, Changsha 410083, China

Received 20 June 2024; accepted 22 August 2024

Abstract: Due to a series of exceptional properties, titanium and titanium alloys have received extensive attention in recent years. Different from other alloy systems, there are two allotropes and a sequence of metastable phases in titanium alloys. By summarizing the recent investigations, the phase transformation processes corresponding to the common phases and also some less reported phases are reviewed. For the phase transformation only involving α and β phases, it can be divided into $\beta\rightarrow\alpha$ transformation and a reverse transformation. The former one has been demonstrated from the orientation relationship between α and β phases and the regulation of α morphology. For the latter transformation, the role of the stress has been discussed. In terms of the metastable phases, the mechanisms of phase formation and their effects on microstructure and mechanical properties have been discussed. Finally, some suggestions about the development of titanium alloys have been proposed.

Key words: titanium alloys; phase transformation; microstructural evolution; mechanical properties

1 Introduction

Over the past 30 years, titanium and titanium alloys have experienced an unprecedented development in many fields, ranging from aerospace industry to biomedical applications [1,2]. Their outstanding combination of high specific strength, excellent anti-corrosion ability and other special features has attracted wide attention [1,3]. Unlike other alloys, titanium is an allotropy which can exist in two phases including α phase with hexagonal close packed (HCP) lattice structure at low temperature and β phase with body-centered cubic (BCC) lattice structure at high temperature. Therefore, different microstructures can be obtained by regulating the size, morphology and distribution of the two phases in various conditions. According to the geometry of α phase, the microstructures of α+β titanium alloys can be classified into four kinds: equiaxed microstructure, bimodal microstructure, Widmanstätten microstructure and basket-weave microstructure [2]. RAN et al [4] reported that the basket-weave microstructure has the highest strength but the lowest plasticity, while the Widmanstätten microstructure is the opposite. The bimodal microstructure has the advantages of the former two, with the optimal combination of strength and plasticity. By understanding the forming conditions of α phase with different characteristics and their influence on the properties, the processing−microstructure−property relationship can be built and thus provides basic guidance to the further fabrication of titanium alloys with promising properties.

The $\beta\rightarrow\alpha$ equilibrium phase transition can be achieved by slow cooling from the β phase field. The allotropic transition between β and α is the most common, and most complete phase transition process in titanium alloys. However, a series of

Corresponding author: Ji GU, Tel: +86-15116333369, E-mail: guji9219@csu.edu.cn;
Min SONG, Tel: +86-18673113927, E-mail: msong@csu.edu.cn
DOI: 10.1016/S1003-6326(24)66597-0

metastable phases may also be generated during the $\beta\rightarrow\alpha$ transition, as shown in Table 1. The firstly generated metastable phase may be β' phase with lean β stabilizers through β phase separation [5,6]. Other phases include martensitic α'' (orthogonal structure) [7,8], martensitic α' (HCP structure) [9,10], intermediate ω phase (hexagonal structure) [11,12] and some uncommon phases such as FCC phase [13,14], O' [15,16] and O'' phases [17,18]. The crystal structures of the metastable phases are between the BCC structure of β phase and the HCP structure of α phase (as shown in Table 1). On the other hand, the reverse transformation from these metastable phases to the equilibrium α phase and β phase can also be achieved under certain conditions. In reality, the reverse transformation in titanium alloys is very common, such as the α''-to-β transformation [19] and ω-to-β transformation [12].

Table 1 Various phases in titanium alloys and their crystalline structures

Phase	Crystalline structure
β	Body-centered cubic structure
α	Hexagonal close packed structure
β'	Body-centered cubic structure
α'	Hexagonal close packed structure
α''	Orthogonal structure
ω	Hexagonal structure
FCC	Face-centered cubic structure
O'	Hexagonal structure
O''	Hexagonal structure

In order to improve the mechanical properties of titanium alloys, all kinds of deformation methods have been adopted by researchers, including rolling, compression, forging and so on [20,21]. The introduction of stress during plastic deformation would inevitably result in various phase transformations, including not only the formation of equilibrium phases but also the metastable phases mentioned above [2,21]. Therefore, it is crucial to understand the phase transformation processes under different processing conditions and also their effect on the alloy properties. ZHANG et al [1] utilized an inevitable presence of interstitial atoms (O and N) to regulate the microstructural variables of the α-precipitation at GBs during the thermomechanical and subsequent heat treatment processes, and an ultra-high yield strength of ~1800 MPa was achieved by this grain boundary engineering strategy for a low-cost titanium alloy [1]. Besides, ZHANG et al [21] acquired a high density of coherent α'/β phase boundaries via martensite transformation induced by thermo-mechanical process and conferred the Ti−2.8Cr−4.5Zr−2.5Al alloy a combination of high strength, ductility and toughness. By elaborate manipulation, the stress-induced α'' martensite transformation (SIM α'') has been controlled by LI et al [7] and brought a high work-hardening ability together with high tensile strength (1215 MPa) and uniform elongation (11%) for Ti−6Al−4V−5.5Cu (wt.%) alloy. Moreover, it is worth noting that each processing often involves more than one type of phase transformation due to the complexity of titanium alloys. In the study of GUAN et al [22], stress-induced martensite transformation occurred during the early deformation stage, causing significant work hardening. And in the latter deformation process, α phase nucleated at the boundaries between α'' martensite and β phase, making another peak of work-hardening. Therefore, it can be found that the metastable phases can act as the intermediary to induce the formation of α phase. With the exception of α'' phase, ω phase has also been found to assist nucleation of α phase [11,23].

This review is to describe the recent progress on phase transformations in titanium alloys in different processing conditions. The various phases and their formation mechanisms, and their effect on microstructure evolutions and mechanical properties are discussed.

2 Allotropic transformation

2.1 $\beta\rightarrow\alpha$ transition

The low-temperature stable α phase in titanium alloy can be precipitated directly from β matrix through high-temperature aging process. Because the high-temperature aging process provides sufficient driving force for $\beta\rightarrow\alpha$ phase transformation, it is seldom accompanied by the generation of metastable phase.

2.1.1 Orientation relationship and variant selection

It is generally believed that the orientation relationship (OR) between α and β phases conforms to Burgers orientation (OR): $(0001)_\alpha//(110)_\beta$ and $[11\bar{2}0]_\alpha//[111]_\beta$, as shown in Fig. 1(a) [24]. The

Burgers OR not only affects the orientation of α phases, but also affects the morphology of α phases. It has been shown that the α phase conforming to Burgers OR is usually lamellar and grows along a lattice invariant line of $\langle 335\rangle_\beta$, with a specific habit plane $\{334\}_\beta$ or $\{11\ 11\ 13\}_\beta$ [25].

According to the characteristics of the Burgers OR between the two phases and the symmetry of the β matrix, twelve possible α phase variants can be generated from a single β grain, and several specific axis/angle relationships are maintained among the α phase variants within the same β grain [26]. In general, the formation probability of these twelve α variants should be equal. However, in most fabrication process, the probability of occurrence of one or some specific α variants can be much greater than that of others. This phenomenon is known as variant selection [26]. In recent years, many studies have been carried out on variant selection during the $\beta\rightarrow\alpha$ transformation through a combination of experiments and simulations, and the results show that it can occur in various types of titanium alloys.

The primary α phase [27], special β grain boundary [28] and dislocation in β phase [29] are the main factors contributing to variant selection. For example, different α variants own different degrees of elastic self-accommodation when contacting with each other, and the interfacial energies are also different for different α variants when interacting with grain boundaries [30]. It has been shown that the lamellar α phase in basket-weave microstructure has a tendency to form the clusters consisting of three α variants [2]. And these three α variants have the same $\langle 11\bar{2}0\rangle_\alpha$ axis parallel to $\langle 111\rangle$ of the β matrix (Figs. 1(b−d)) [11]. This microstructure is considered to be generated due to the accommodation of transformation strain of one variant from others [2]. It is worth noting that the selection of α phase variant has a negative effect on the mechanical properties of titanium alloys such as strength, plasticity and fatigue [31,32]. BHATTACHARYYA et al [33] analyzed the effect of the crystallographic misorientation between two adjacent β grains on variant selection. The results show that α phase at the grain boundary

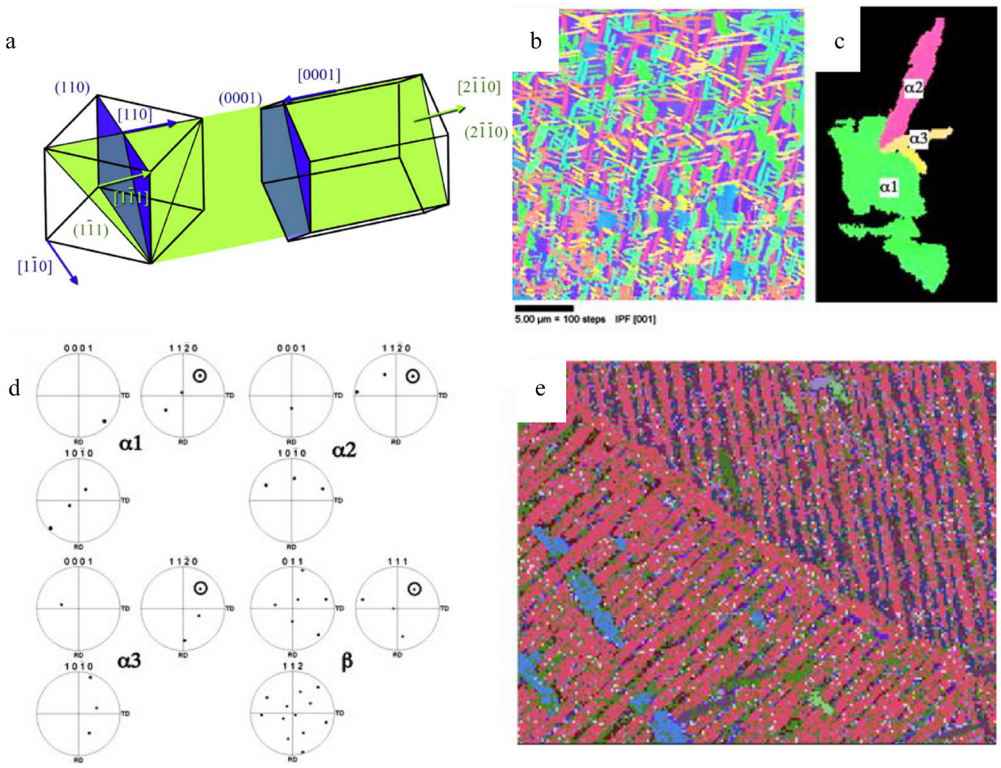

Fig. 1 Burgers orientation relationship between BCC-β phase and HCP-α phase (reproduced with permission from Ref. [24], Copyright (2017), Elsevier) (a); OIM images of three variants with same $\langle 11\bar{2}0\rangle_\alpha$ axis parallel to $\langle 111\rangle$ of β matrix (reproduced with permission from Ref. [11], Copyright (2009), Elsevier) (b−d); Length of α at grain boundary and lamellar α with same crystallographic orientation growing into adjacent β grains (reproduced with permission from Ref. [33], Copyright (2007), Elsevier) (e)

has a coherent OR with the β grains on both sides, and even has the same crystallographic orientation with the α colonies within both adjacent β grains (Fig. 1(e)). Therefore, the α colonies within both adjacent β grains and α phase at the grain boundary can be considered as a whole colony with the increase in crystallographic size compared with the former one. This increases the effective slip path of the dislocation during deformation and decreases the strength and fatigue properties of the alloy [33].

With the exception of classical Burgers OR, MATSUKAWA et al [24] also concluded several other ORs between HCP phase and BCC phase, including Pitsch−Schrader OR [34], Potter OR [35], Rong−Dunlop OR [36] and Zhang−Kelly OR [37]. The OR between β phase and α phase found in the as-cast Ti-55511 titanium alloy follows the Potter OR: $\{110\}_\beta//\{10\bar{1}1\}_\alpha$, $\langle 111\rangle_\beta//\langle 11\bar{2}0\rangle_\alpha$ [35]. And the result shows that the (0001) plane in α phase deviates ~6° from the {110} planes, while $(10\bar{1}1)$ plane is closer to the {110} planes [35]. The Pitsch−Schrader OR, which has a deviation of 5.3° from the Burgers OR, has also been observed in a hot-rolled titanium alloy [34]. For the deviation between Burgers OR and other ORs, it is generally considered to be the result of alloy concentration and deformation degree [38].

2.1.2 Spheroidization mechanisms of α phase

The main resource of strength, together with strain incompatibility and stress inhomogeneity, in titanium alloys is the hindrance to dislocation slip provided by α/β interfaces [39]. Therefore, tailoring the morphology, size and distribution of α phases in titanium alloys to obtain excellent mechanical properties by controlling $\beta\rightarrow\alpha+\beta$ phase transformation is of significant importance and has been the research focus for a long time. The α phase usually exists in two forms: the equiaxed α phase and the lamellar α phase [40]. The latter is a result of cooling from temperatures above the β-transus temperature [40], while the equiaxed microstructure corresponds to the recrystallization process [41]. Various combinations of lamellar and equiaxed α phases can form different microstructures with outstanding mechanical property. ZHANG et al [1] reported that the ultra-high yield strength of a low-cost duplex titanium alloy can be enhanced to ~1800 MPa by hierarchically heterogeneous microstructure composed of micron-scaled primary α, nano-scaled secondary α and ultrafine Widmanstätten α phases in the β-matrix. Another hierarchical nanostructure consisting of uniformly-distributed and micro-sized α precipitates was obtained in Ti-185 alloy with the yield strength of 1655 MPa by DEVARAJ et al [42].

Different from the formation of the lamellar α phase, obtaining equiaxed α phase requires large enough plastic deformation in the $\alpha+\beta$ region and subsequent annealing. In other words, the formation of equiaxed α phase involves the spheroidization of the lamellar α phase. The spheroidization of lamellar α can be divided into two processes: the dynamic spheroidization during deformation and the static spheroidization during heat treatment [3,43−45]. By considering various conditions of deformation and heat treatment, spheroidization process is extremely complicated since the dynamic and static processes overlap. The dynamic spheroidization is an essential microstructure evolution behavior during the thermomechanical process occurring in titanium alloys. A series of investigations referring to dynamic spheroidization of lamellar structure have been carried out, and mainly focus on the microstructural evolutions, the spheroidization mechanisms and the influences of spheroidization on mechanical properties [44,46]. Until now, various spheroidization mechanism models have been proposed including boundary splitting model, edge spheroidization model, laths shearing model, continuous dynamic recrystallization model and so on [47−51]. For the boundary splitting model, the lamellar α phase experiences shear deformation firstly due to the external force, and some grain boundaries slip to produce unstable interfaces. Since the unstable interface has high energy, the element diffusion is easy to occur at high temperature, resulting in the β phase wedging into the lamellar α phase, forming a new α/β interface, and the lamellar structure will isolate a spherical structure to achieve the purpose of spheroidization. Similarly, the diffusion of β-phase stabilizing elements into lamellar α phase from the high-energy defects were also found in edge spheroidization model [52]. Different from the former two models, the function of β phase is not shown for laths shearing model [48].

Although the mechanisms are different, according to the characteristics of dynamic spheroidization, the process can be divided into three stages: the formation of high-energy

structures, the instability of lamellae induced by the high-energy structures, and the coarsening process [47]. The existence of the first stage indicates that the occurrence of spheroidization needs a preparation stage. In fact, the dynamic spheroidization of lamellar α occurs only when the strain of specimens reaches the critical point [53]. SEMIATIN et al [53] reported that the critical strain of dynamic spheroidization was approximately 0.75−1.0 when the Ti−6Al−4V titanium alloy with lamellar microstructure was deformed at 815 and 955 °C with the deformation rate of 0.001 s^{-1}. The lamellar α of titanium alloy owns excellent stability, and thus it is not easy to obtain the complete spheroidization microstructure only by dynamic spheroidization [54]. Therefore, heat treatment after deformation to achieve static spheroidization has become an important way to obtain the complete spheroidization structure. ZHEREBTSOV et al [51] reported that the spheroidization mechanisms would change corresponding to the temperature. They conducted the heat treatment at 600 and 800 °C on the Ti−6Al−4V alloy after isothermal compression and found that at 800 °C, the fragmentation of lamellar α was caused by boundary splitting mechanism. However, at 600 °C, the continuous dynamic recrystallization and static recrystallization were the main mechanisms to determine the microstructure evolution [51].

2.2 $\alpha\rightarrow\beta$ transformation

Apart from the phase transformation from $\beta\rightarrow\alpha$, the reverse transformation from β phase to α phase has also been investigated widely. Commonly, the $\alpha\rightarrow\beta$ phase transformation is the result of raising the temperature from α or $\alpha+\beta$ region to β phase region. This process is determined by the diffusion transfer of slow β-phase stabilizing elements, such as V and Mo atoms, from α to β. It is worth noting that the $\alpha\rightarrow\beta$ phase transformation can also be affected by various conditions similar to the $\beta\rightarrow\alpha$ phase transformation. According to the conventional kinetics theory for the diffusion-controlled phase transformation, the reverse transition should be slower than the temperature rise with the increase in heating rate [55]. Therefore, the β-transus temperature shows an increase trend with raising the heating rate. However, ZHOU et al [15] found the β-transus temperature dropped by 50 °C during the research on the $\alpha\rightarrow\beta$ phase transformation via electropulsing treatment. This phenomenon is the result of the action of stress, including thermal and mechanical stress.

The phase transition is a transformation process of two energy systems. From the perspective of dynamics, the phase transition requires a certain driving force. The driving force of the phase transition without the function of strain is the free energy difference generated by the two phases when the temperature is changed. However, in the thermal deformation process, the work done by the deformation stress may provide driving force for the phase transition. In addition, since the diffusion conditions and distribution characteristics of solute elements during the deformation process are different from those in the non-deformed process, the two-phase equilibrium state is changed, which may promote or inhibit the phase transition. The tensile deformation of Ti−5.5Al−1Fe alloy at 1050−1200 K was carried out by KOIKE et al [56], and it was found that Fe element was redistributed in the α and β phases under the action of stress. Due to the change of Fe element distribution, the free energy of the two phases was changed, and the free energy increased for the α phase and decreased for the β phase, thus promoting the $\alpha\rightarrow\beta$ transition. Some studies have also shown that the $\alpha\rightarrow\beta$ phase transition in titanium alloys can be inhibited under certain stress. LIU et al [57] found during the forging deformation process of Ti−1.5Fe−2.25Mo alloy below the β-transus temperature, the transformation degree from α to β decreased obviously with the increase in the deformation degree. They reported that the energy stored during deformation process can change the phase equilibrium state, resulting in the restrictions of α-to-β transformation.

3 Metastable phase transformation

It has been found that a series of metastable phases can precipitate from the β matrix, such as β', α', α'', ω, O', O'' and other phases, by regulating the stability of β phase in titanium alloys under different heat-treatment and deformation conditions.

3.1 β' phase transformation

Recently, a new avenue has been opened up by

chemical boundary engineering for the production of hierarchically heterogeneous microstructures in alloys, including magnesium alloys and steels. By using chemical discontinuity within continuous lattice regions (such as spinodal decomposition structure), excellent combinations of strength and ductility can be achieved [58,59]. Spinodal decomposition refers to the process of spontaneous separation of a homogeneous phase into two or more coexisting phases with the same crystal structure but different compositions through non-nucleated uphill diffusion. In fact, phase separation based on spinodal decomposition mechanism has been observed in a variety of titanium alloys, especially for metastable β-Ti alloys [60,61]. This results in the formation of two solid solutions: the β phase with more β-stabilizers and the β' phase with less β-stabilizers. The two phase are sometimes named as β_1 and β_2 [6]. In addition, the interface between β phase and β' phase is coherent.

In terms of distinguishing the two phases, X-ray diffraction (XRD) and transmission electron microscopy (TEM) analysis are considered to be the effective ways [2]. AFONSO et al [62] adopted monochromatic synchrotron radiation to obtain the XRD pattern of aged Ti−35Nb−7Zr−5Ta alloy, as shown in Fig. 2(a). It can be seen that an apparent peak split exists at the (101) diffraction peak, meaning the occurrence of β phase separation. Combined with other characterizations, AFONSO et al [62] pointed out that the splitting of diffraction peak was caused by the lattice parameter distortions induced by the composition fluctuations of heavy elements (Ta and Zr). TEM observations were conducted by YANG et al [5] on a metastable β titanium to study the phase transformation referring β' phase, and some of the results can be seen, as shown in Figs. 2(b−e). In Fig. 2(b), HAADF (high-angle annular dark-field)-STEM (scanning transmission electron microscopy) image of the striation structure was obtained, and the contrast difference means the alternate distribution of β phase and β' phase. Energy dispersive spectrometer (EDS) results of the formed striation structure show that the segregation of V and Ti elements occurred

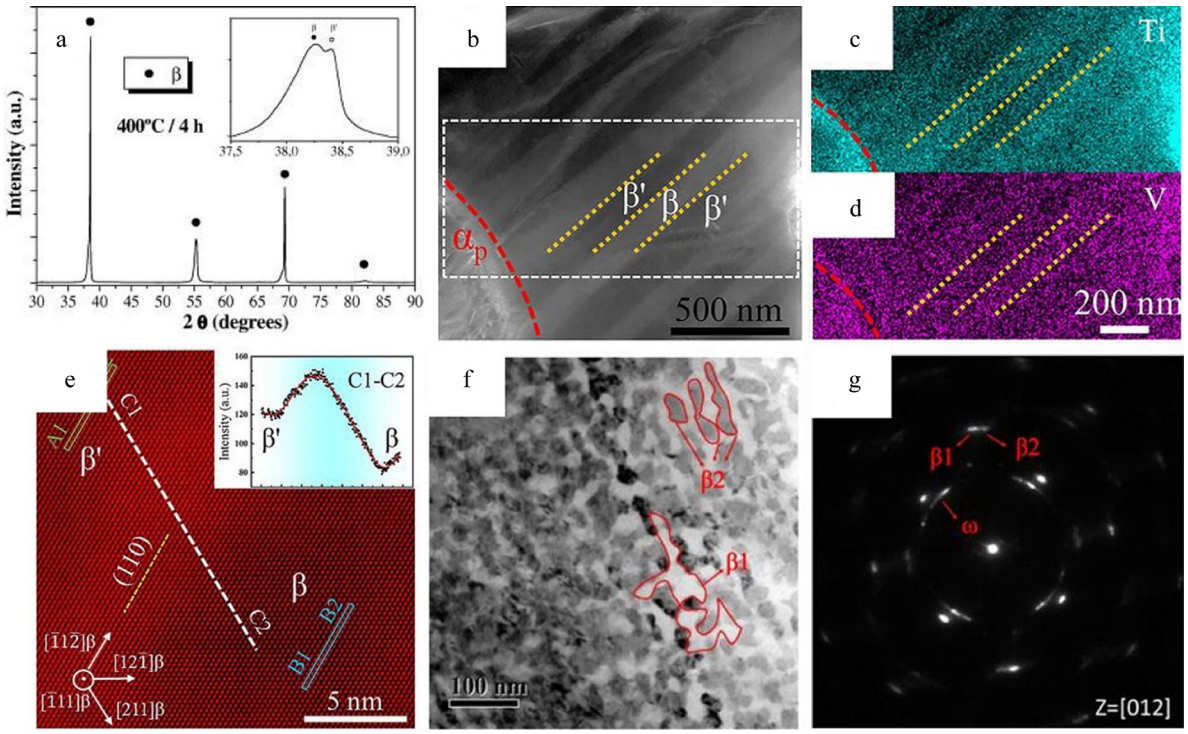

Fig. 2 XRD pattern of Ti−35Nb−7Zr−5Ta alloy (reproduced with permission from Ref. [62], Copyright (2010), Elsevier) (a), HAADF-STEM image of striation structure in Ti−4.5Al−4.5Mo−7V−1.5Cr−1.5Zr alloy (reproduced with permission from Ref. [5], Copyright (2024), Elsevier) (b); EDS maps of region framed by dotted white line in (b) (reproduced with permission from Ref. [5], Copyright (2024), Elsevier) (c, d); Interface of β and β' in (b) (reproduced with permission from Ref. [5], Copyright (2024), Elsevier) (e); TEM images of aged Ti−40Zr−12Ta alloy (reproduced with permission from Ref. [6], Copyright (2023), Elsevier) (f, g)

in β phase and β' phase (Figs. 2(c, d)), respectively. Besides, the atomic structure of a coherent β/β' interface can be observed in Fig. 2(e) along $[\bar{1}11]_{\beta}$. And the integrated intensity of atomic columns along the white line from β' phase to β phase was plotted in the inserted image, and shows a gradual intensity change in accordance with the result of AN et al [63]. The phenomenon of β phase separation was also found by XIAO et al [6] in a Ti−40Zr−12Ta alloy. TEM bright field image showing two phases with different contrasts and the corresponding selected area electron diffraction (SAED) pattern with the splitting of diffraction points can be seen in Figs. 2(f) and (g), respectively. Both of the observations indicate the occurrence of spinodal decomposition, but it is worth noting that the spinodal decomposition takes place in certain conditions. It was observed that the spinodal microstructure existed only in the temperature range of 500−700 °C in the TZT12 alloy, and when the temperature arose to 800 °C, it disappeared. This is probably related to the miscibility gap region of the Ti−Zr−Ta phase diagram [64]. Apart from XRD and TEM analyses, energy-dispersive X-ray spectroscopy is another way adopted by GEORGE and DIVAKAR [65] to quantificationally confirm the compositional fluctuations existing in Ti−15Mo alloy.

The occurrence of spinodal decomposition also has a certain effect on other phase transformation processes. As a metastable phase with segregation of β-phase stabilizing elements, β' phase has been considered as the precursor for the generation of other phases, such as ω phase [61] and α phase [66]. It should be concerned with the gradient strain at the β/β' interface. The β/β' interface can provide stress field for the atom diffusion to accelerate the phase transformation [60,61]. DEVARAJ et al [67] investigated the sequential β-phase separation and subsequent structural transformation from Mo-depleted β regions to ω phase. They pointed out that the strain existing at β/β' interface can provide driving force for the plane collapse during ω nucleation process, and act as preferential sites for diffusion (e.g. solute lean region) to aid ω transformation. In fact, the ω phase has been proven to directly or indirectly assist the nucleation of α phase [68]. YANG et al [5] reported that, at the beginning of aging, β' phase, ω phase and α_s phase existed together. With long-time aging, α_s phase gradually nucleated and grew up with the decrease in the size of β/β' striation structure and ω phase. Finally, striation structure and ω phase disappeared with the only presence of α_s phase, as shown in Fig. 3. With the exception of assisting α nucleation under the help of ω phase, β' phase has also be found to directly aid the formation of α phase. ZHU et al [66] observed the nucleation of α phase occurring at the β/β' interface and subsequent growth of the α phase into the β' phase.

β' phase plays an important role in the mechanical properties of titanium alloys. By considering the interface between β phase and β' phase, the boundary strengthening effect can be achieved through the pile-up of dislocations at the interfaces. The β-spinodal structure with an average width of ~122.6 nm was calculated to provide ~165.7 MPa increment in the tensile yield stress [5]. In fact, the strength increment $\tau_{spinodal}$ comes from two contributions [69]: (1) the misfit effect τ_{ε} from the coherency stress resulted by the periodic variation of the lattice constant, and (2) the modulus

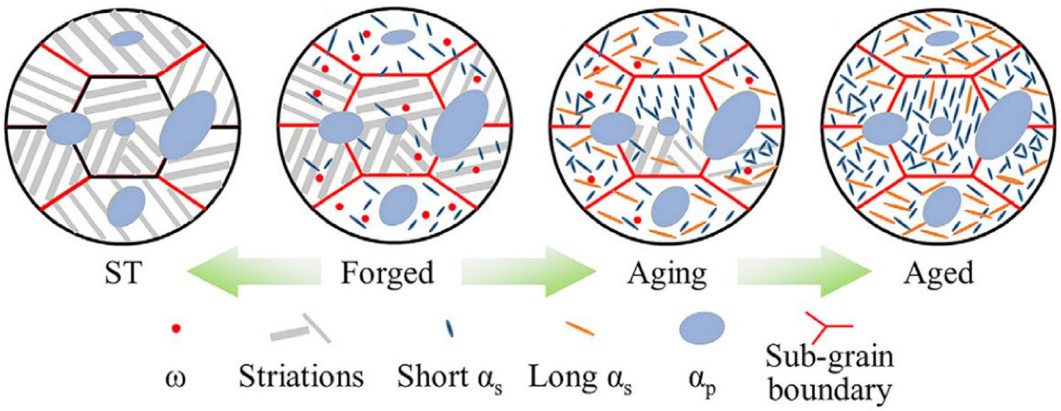

Fig. 3 Schematic diagram of phase transformation pathways in aging process referring to β' (reproduced with permission from Ref. [5], Copyright (2024), Elsevier)

effect τ_G came from the change of elastic moduli related to the composition modulation. Therefore, the reinforcement of the spinodal structure can be calculated by utilizing the formula [70,71]:

$$\tau_{\text{spinodal}} = \tau_{\varepsilon} + \tau_{G} = \frac{A\eta E}{2(1-\upsilon)} + \frac{0.65\Delta G b}{\lambda_s} \quad (1)$$

where A is the amplitude of compositional fluctuation, η is the variation of the lattice constant, E is the elastic modulus, υ is the Poisson's ratio, ΔG is the difference in shear moduli between β and β' striations, b is the magnitude of Burgers vector, and λ_s is the wavelength of the spinodal structures. Moreover, β' phase can indirectly affect the mechanical properties of titanium alloys via playing a role in various phase transformations mentioned above [60,70]. By considering the influence of β' phase on microstructural evolutions and mechanical properties of titanium alloys, it is essential to further study the specific mechanisms of β' phase transformation and try the best to control the phase transformation process to strengthen the materials. The existence of β' phase can also bring about outstanding plasticity. The periodically spaced stripe structure in a HfNbTiV alloy reported by AN et al [63] can act as hurdles to change the slip mode of the dislocations and result in a high tensile strain to failure (28%).

3.2 α' and α'' phase transformation

The martensite transformation in titanium alloys refers to the transformation from β phase to martensite phases, including HCP α' phase and orthogonal α'' phase. The formed α' and α'' phases are both supersaturated solid solution. These phase transformations without element diffusion are caused by atomic shear with rapid transition speed. In fact, the martensite transformation is an intermediate process of the $\beta \rightarrow \alpha$ transformation, and the generated martensite phase is determined by the lattice resistance related to the content of β-phase stabilizing elements. For the titanium alloys with less β-phase stabilizing elements, the α' phase will be formed. However the α'' phase will be obtained in the titanium alloys with more β-phase stabilizing elements [72]. The occurrence of martensite transformation needs high supercooling or mechanical stress. In other words, the generation of α' and α'' phases tends to take place in quenching and various deformation processes [2]. The phase transformation induced by deformation is called stress-induced martensitic transformation (SIMT) [8,10]. This phenomenon was first discovered in the transformation-induced plasticity steel [73]. During the deformation of the steel, the residual austenite was transformed into martensite, and the volume change resulted by the phase transformation consumed certain applied stress, and thus improved the fracture toughness of the steel. Similarly, the generation of α' and α'' phases induced by applied stress can also relieve stress concentration in titanium alloys [73,74]. NIINOMI et al [73] reported that SIMT phenomenon was an effective way to improve the fracture toughness of Ti−6Al−4V alloy and SIMT also improved the fracture toughness of Ti−10V−2Fe−3Al alloy [74].

The α' phase tends to appear in near-α or α titanium alloys, having the same crystal structure as α phase [75]. Typically, both α and α' phases keep the Burgers OR with β phase as $(0001)_{\alpha/\alpha'}//(110)_{\beta}$, $[11\bar{2}0]_{\alpha/\alpha'}//[111]_{\beta}$ [38]. In addition, there may be other ORs for α/α' phase and β phase, such as Pitsch−Scharder OR [24]. Therefore, it is difficult to distinguish α phase and α' phase by general detection and characterization. However, the difference of generation conditions is considered as an usual way to distinguish the two phases [2]. The crystal structures of α'' phase and α phase are different, so the distinction between the two phases is easy to observe during the detection and characterization [7]. And the OR between α'' phase and β phase is $(001)_{\alpha''}//\{110\}_{\beta}$, $\langle 100\rangle_{\alpha''}//\langle 100\rangle_{\beta}$ [76], different from both α phase and α' phase.

3.2.1 Stress-induced martensite

There are two types of martensitic phase in titanium alloys, including the stress-induced martensite and athermal martensite, obtained from the metastable β phase by deformation and cooling, respectively [8]. The formation of isothermal α' and α'' phases were also reported recently during isothermal aging [77].

By considering the formation of stress-induced martensite (SIM), there are many affecting factors including deformation temperature, β phase stability, β grain size, strain rate and so on [78]. According to the Clausius−Clapeyron equation [79], the higher the deformation temperature, the greater the SIM phase transformation critical stress. Additionally, the β phase stability can also be enhanced by raising the deformation temperature, causing the difficulty

in inducing the SIM. XU et al [78] studied the deformation mechanism of a Ti−Nb−Ta−In/Cr alloy during the deformation process, and found that the β phase stability of the alloy was also changed with the change of alloy element content, which led to the change of alloy deformation mechanism. The results show that in the Ti−Nb−Ta−In alloy with low β phase stability, multiple deformation mechanisms including stress-induced martensitic transformation, twinning and dislocation slip exist, while dislocation slip is the only deformation mechanism for Ti−Nb−Ta−Cr alloy with high β phase stability. The size of the β grains also has a large influence on the stress-induced martensitic phase transition. BHATTACHARJEE et al [80] found that the larger the β grain, the lower the critical stress of the SIM phase transition. However, it has been found in the as-solution treated Ti−10V−2Fe−3Al alloy that the critical stress of α'' martensite generation increased from 290 to 533 MPa with the grain size increasing from 130 to 300 μm [80]. This is mainly because the effect curve of grain size on the critical induced stress of martensite has a U-shape, indicating that the critical stress reaches a minimum value at an intermediate point [81]. Strain rate is also an important parameter affecting the SIMT. AHMED et al [20] found that at low strain rate (10^{-3} s^{-1}), the main deformation mechanism was related to the SIM-α'' phase. At a moderate strain rate (10^{-1} s^{-1}), the main deformation mechanism involved the competition between the SIMT and {332}⟨113⟩ twinning. However, at the high strain rate (10 s^{-1}), {332}⟨113⟩ twinning was the only dominant mechanism due to high strain rate providing a high density of dislocations that promoted twinning while suppressing the SIMT.

The SIMT has been verified to affect the mechanical properties of titanium alloys by various ways [8,82]. JIA et al [8] found the presence of SIM-α' resulted by the tensile deformation with 4% strain in a quenched Ti−2.8Cr−4.5Zr−5.2Al alloy. Though the SIM sometimes would sacrifice the yield strength for titanium alloys, it can act as the intermediary to form other structures to strengthen the materials. In the work of JIA et al [8], the lamellar SIM-α'' finally transformed into the ladder-like α_s during the subsequent aging process, resulting in the increase in both yield and tensile strength. Besides, the SIM can also cause a significant improvement in the ductility of titanium alloys. For example, an outstanding combination of high tensile strength (~1 GPa) and uniform elongation (>38%) was achieved under the function of SIM-α'' in a metastable titanium alloy [82].

Similar to α phase, the martensites including α' phase and α'' phase also have various variants which can cause remarkable effect on the performance of titanium alloys [9,83]. In fact, there are several studies reporting the reorientation induced plasticity (RIP) of martensite in titanium alloys [9,83]. DUMAS et al [9] investigated the reorientation behavior of α' martensite, and the reconstructed variants can be seen in Fig. 4(a). In their work, it was shown that RIP was induced by the movement of an unusual twin interface among martensite variants in the same self-accommodating groups. And it was the first one to prove that the motion of twin interface occurs not only in the α'' martensite, but also in the α' martensite. Moreover, during the deformation, there are also some substructures forming in the SIM [10]. It can be observed in Figs. 4(b, c) that both the deformation twins and stacking faults were generated within the SIM-α', resulting in the combined effect of transformation induced plasticity and twinning induced plasticity on the strain hardening [10].

In addition, it is worth noting that there is a special feature that can be found from the strain-stress curves like Fig. 4(d) [22]. Different from general strain−stress curves, these curves have two yield points and the phenomenon is called double-yielding effect. In fact, the first yield point is caused by the generation of SIM and the second yield point is related to the common plastic deformation of matrix [84]. GUAN et al [22] investigated the deformation mechanisms of different deformation stages with the adiabatic shear band, and the related mechanisms can be seen in Fig. 4(e). During the tensile process, the accumulation of the stress induced the formation of SIM-α'' corresponding to the first plateau of strain−stress curve and the α'' deformation twins were subsequently introduced to accommodate the transformation strain. Finally, the α phase nucleated at various high-energy boundaries with the α twinning being induced subsequently, and the microstructure reached dynamic equilibrium.

3.2.2 Athermal martensite

Except for SIM, athermal martensite obtained

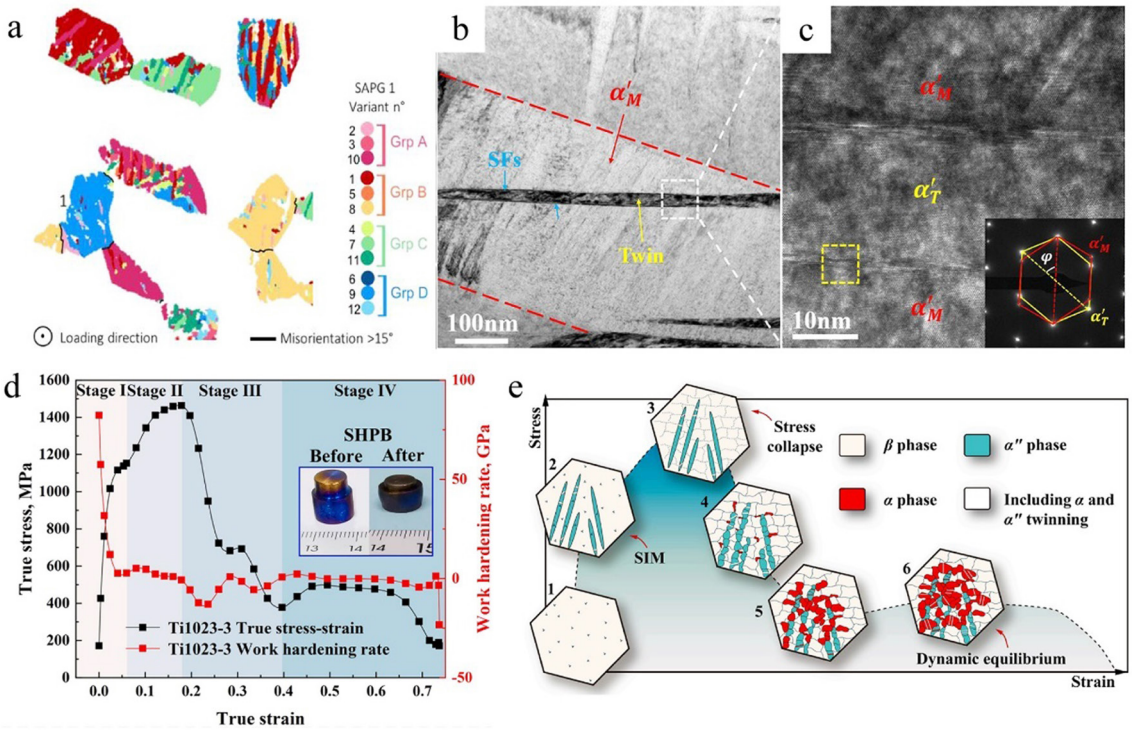

Fig. 4 EBSD map of α' martensite variants in deformed Ti−6Al−4V alloy (reproduced with permission from Ref. [9], Copyright (2021), Elsevier) (a); TEM images of α' martensite with substructures (reproduced with permission from Ref. [10], Copyright (2023), Elsevier) (b, c); True stress−strain and strain hardening rate curves of Ti-1023 alloy obtained from split Hopkinson pressure bar test (d), and corresponding schematic diagram of microstructural evolution within adiabatic shear band (e) (reproduced with permission from Ref. [22], Copyright (2023), Elsevier)

by water quenching also plays an important role in breaking the strength−toughness trade-off dilemma for titanium alloys [21]. It is known that the precipitation of α phase with dense α/β interfaces can significantly strengthen the titanium alloys, but together with the drop in ductility and toughness [85]. The reason for this condition is that when plenty of dislocations piled up at the semi-coherent α/β interfaces, severe stress concentrations can be caused, thus resulting in the failure of materials. To avoid this dilemma, ZHANG et al [21] introduced a great number of three-ordered athermal α' martensite with coherent α'/β interfaces (Figs. 5(a−d)), and the results show that the hierarchical nanomartensite microstructure owns an outstanding combination of ultimate tensile (~1411 MPa) and elongation (~12.1%). It is worth noting that different from the brittle α' martensite, orthorhomibic α'' martensite is softer. Though the introduction of α'' martensite would reduce the yield strength, it can also bring higher ultimate tensile strength [7]. The extraordinary strain-hardening ability of athermal α'' martensite was adopted by LI et al [7] to reduce the risk of cracking during subsequent cold deformation. This characteristic of α'' martensite provides an effective solution for the titanium alloys with high deformation resistance at low temperature.

3.2.3 Isothermal martensite

As for the isothermal α'' phase, it has been received extensive concern as a key precursor to form stable equilibrium α and β phases [86,87]. An isothermal α'' phase was observed in a metastable titanium alloy after isothermal aging [88]. Different from the forming mechanism related to the nucleation from SIM and athermal martensite, TAHARA et al [88] found that the isothermal α'' phase was formed due to the upset of balance among nanodomains, which had suppressing effect on the generation of martensite [89]. In fact, the formation of isothermal α'' phase referred to a short-range atomic rearrangement, and the composition change was not found in the transformation from isothermal α'' phase to α phase manifesting with no relation to precipitation and spinodal decomposition [89]. Actually, various

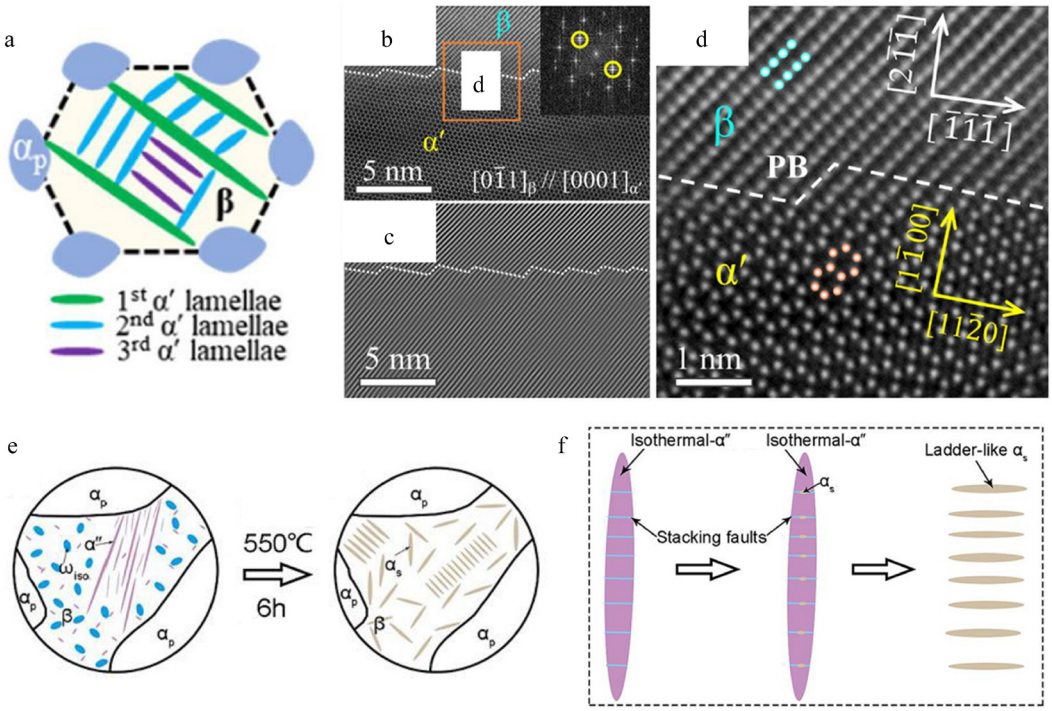

Fig. 5 Schematic diagram of microstructural features with three-ordered athermal α' martensite for water-quenched Ti−2.8Cr−4.5Zr−2.5Al alloy (reproduced with permission from Ref. [21], Copyright (2024), Elsevier) (a); TEM images showing coherent α'/β phase boundary (PB) (reproduced with permission from Ref. [21], Copyright (2024), Elsevier) (b−d); Schematic illustration of microstructure evolution during aging process at 550 °C for 6 h (e) and transformation from isothermal α'' with stacking faults to ladder-like α_s (f) (reproduced with permission from Ref. [8], Copyright (2024), Elsevier)

pathways leading to the precipitation of α phase induced by diffusion-based isothermal α'' phase were reported by researchers [8,90]. It can be seen from Figs. 5(e, f) that the transformation from isothermal α'' phase to ladder-like secondary α phase occurred with the help of stacking faults during the aging process in Ti−3Al−5Mo−4.5V alloy [8]. And it was found that the critical structure is the interface of α'' phase and β matrix with chemical composition fluctuation and stress gradient which can act as the sites for the nucleation of α phase [91].

3.3 ω phase transformation

3.3.1 Classification of ω phase

The ω phase is also a common metastable phase in titanium alloys. Figure 6(a) shows the schematic illustrations of the transformation from β to ω [92]. It is clear that the transformation is related to the collapse of {111} planes. Specifically, during the β to ω transformation, the first and fourth {111} planes keep unchanged with the middle two planes collapse and form a new plane. And the presence of ω phase is usually verified by the extra diffraction points at 1/3 and 2/3 $\{112\}_\beta$ locations along $[113]_\beta$ zone axis, as shown in Fig. 6(b) [92].

Similar to α' and α'' martensites, ω phase can also be classified into three types according to the formation conditions: athermal ω phase, isothermal ω phase and stress-induced ω phase [2]. The athermal ω phase induced during quenching process usually appears as small ellipsoid (as shown in Fig. 6(c)), which is clearly different from the α' and α'' martensite phases with lath-shaped morphology in titanium alloys [93,94]. Because the formation of athermal ω phase via atomic shuffling is diffusionless and displacive, the athermal ω phase possesses the same composition with β matrix [95]. The formation of isothermal ω phase in aging process is considered as a diffusion phase transition, resulting in a certain difference of the composition between isothermal ω phase and β phase [96]. Therefore, the isothermal ω phase can be achieved from the athermal ω phase by long-time aging [97].

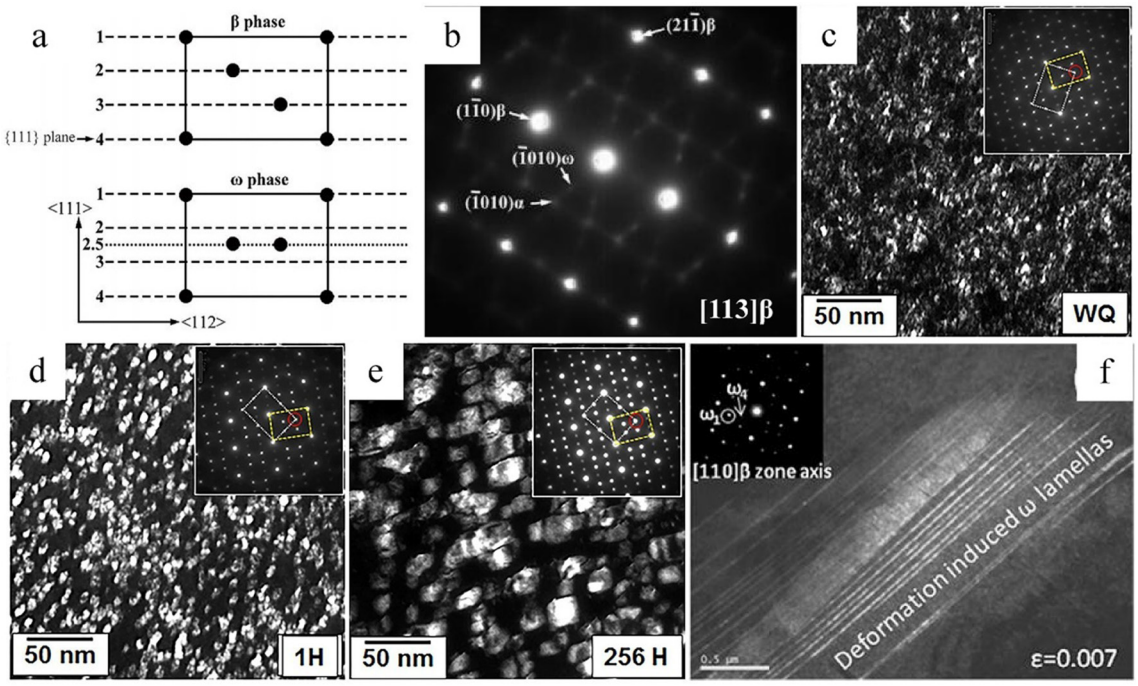

Fig. 6 Schematic illustrations of transformation from β phase to ω phase (reproduced with permission from Ref. [92], Copyright (2017), Elsevier) (a); SAED pattern showing reflections of ω phase at 1/3 and 2/3 $\{112\}_\beta$ (reproduced with permission from Ref. [92], Copyright (2017), Elsevier) (b); Dark-field (DF) TEM images of ω phase with various sizes and morphologies of small ellipsoidal (reproduced with permission from Ref. [94], Copyright (2017), Elsevier) (c), ellipsoidal (reproduced with permission from Ref. [94], Copyright (2017), Elsevier) (d), cubic (reproduced with permission from Ref. [94], Copyright (2017), Elsevier) (e) and lath-like shape (reproduced with permission from Ref. [105], Copyright (2013), Elsevier) (f)

But unlike the conventional nucleation and growth mechanism, isothermal ω phase can grow rapidly even at low temperature [98]. Determined by the lattice misfit, the shape of isothermal ω phase has two types: ellipsoidal shape for low lattice misfit systems obtained from short-time aging and cubic shape for high lattice misfit systems obtained from long-time aging, as shown in Figs. 6(d, e) [94]. These two kinds of ω phases tend to distribute dispersedly in the β matrix, resulting in the increase in strength and decrease in plasticity [99,100].

Different from the former two types, the stress-induced ω phase usually has the lath-like shape (Fig. 6(f)) and provides the improvement in mechanical properties for titanium alloys by transformation induced plasticity effect [101,102]. Moreover, due to the similar atomic shear, the stress-induced ω phase is usually generated accompanied with the formation of $\{112\}\langle 111\rangle_\beta$ twins [103], causing the zigzag configuration of β twins and stress-induced ω phase [104,105].

Furthermore, a ω-like structure named embryonic ω can also be found in β phase before the formation of isothermal ω phase with the evidence of diffuse streaks in diffraction patterns [106,107]. The occurrence of this phenomenon is considered to be an energy-consuming process with the lattice strain reconstruction helping the subsequent generation of ω phase [106]. Therefore, the continuous growth of embryonic ω can be viewed as another formation mechanism of ω phase, which needs to be studied further [108].

3.3.2 New insights into ω phase transformation

During the further studying of ω phase and its related transformation, there are new insights referring to the embrittlement mechanism [109], diffusionless isothermal ω transformation [110] and so on.

It is worth noting that though the precipitation hardening effect of ω phase is remarkable, its inevitable brittleness would also bring about innegligible issue [109]. Therefore, ω phase needs to be avoided in the final state, especially for the engineering materials. And the corresponding

mechanisms of ω phase embrittlement has been widely investigated since 1970s [111,112]. In these early studies, the embrittlement is attributed to the high volume fraction of ω particles in the β matrix impeding primary slip, which promoted secondary slip around each ω particle and finally resulted in the interparticle fracture of ω particles [99,100]. It can be noted that the ω particle is considered to be non-deformable. Afterwards, it is revealed that the dislocation can shear the ω particle, inducing the formation of slip bands [111,112]. These researches ascribed the embrittlement to the high stress concentrations within the slip bands, promoting the crack nucleation [111,112]. It can be concluded that a high volume of ω phase is considered as the key factor to embrittlement in previous studies.

However, there are reports revisiting the embrittlement mechanism of ω phase [82,109]. SUN et al [82] demonstrated that for a Ti−12Mo alloy already containing ductile-ω phase, its ductility is reduced significantly after an aging treatment at 250 °C for 1 min. During aging at such a low temperature with a short time, the volume fraction kept unchanged basically. Therefore, this ductile to brittle transition may be related to the short-range changes of composition. In fact, obvious elemental partition has been observed in ω particles during aging [94,109]. LAI et al [109] reported that the embrittlement was caused by the obvious rejection of Mo element from the ω particles during aging, resulting in a significant increase in shear modulus (>30 GPa) and thus promoting crack nucleation due to the localization of flow stress.

Diffusionless isothermal ω transformation is another newly reported observation in recent years [110,113]. Actually, in titanium alloys containing β-phase stabilizing elements, inevitable compositional fluctuations tend to exist, resulting in the formation of local unstable regions [113,114]. These unstable regions can further induce the diffusionless isothermal ω without the occurrence of athermal ω transformation due to the stable state for the entire β matrix. It is known that for the diffusionless isothermal ω transformation, the kinetics is determined by two processes: dynamic atomic shuffling and a nucleation process. And during the first process, a temporary ω structure can be achieved and then transform into diffusionless isothermal ω phase [113].

3.3.3 Effect of ω phase on mechanical properties

Though the high hardness and brittleness features make ω phase detrimental to the mechanical properties of titanium alloys, the ω phase can act as the medium to assist the uniform and diffuse nucleation of α phase [115,116]. Therefore, the ω phase can improve the mechanical properties of titanium alloys indirectly by regulating the morphology, size and distribution of α phase. LI et al [98] revealed the transformation pathways from embryonic ω to isothermal ω phase and finally to α phase during a long-time aging. From Fig. 7, it can be seen that the whole transformation can be divided into four steps: (1) initially, the spinodal decomposition occurs in β matrix followed by structural reconstruction, forming the embryonic ω (Fig. 7(a)); (2) when the size of embryonic ω reaches a critical point, a diffusive mode will be activated to cause a change in chemistry, resulting in the formation of isothermal ω phase (Fig. 7(b)); (3) the formed O-rich regions at the isothermal ω/β interfaces can be the preferential nucleation sites for α phase (Fig. 7(c)); (4) further diffusion between α and β phases driven by the fast lengthening kinetics enlarges the size of α phase (Fig. 7(d)). Similar ω-assisted α nucleation was observed in a water-quenched TB18 alloy [117]. Based on this, it is reasonable to obtain a uniformly dispersed α phase with outstanding combination of strength and ductility. MANTRI et al [118] significantly improved the ultimate tensile strength of a β-titanium alloy from ~1 to 2 GPa utilizing the precursor ω phase. Besides, appropriate ω-assisted nucleation was adopted by ZHANG et al [117] to suppress the development of continuous grain-boundary α phase and cause the refinement of α lamellae within β grains, resulting in high ultimate tensile strength (~1364 MPa) with excellent ductility (~6.7%).

3.4 FCC phase transformation

In recent research reports, it was found that a phase transformation, from the initial HCP structure to the metastable FCC structure, can be induced in high-purity titanium alloys and α-titanium alloys [119,120]. Due to the excellent deformation ability of FCC structure and the transformation induced plasticity, it is feasible to introduce FCC phase in titanium alloys to improve the plasticity of

materials [121]. Therefore, it is important to explore and understand the mechanism of HCP→FCC phase transformation under different conditions. As far as we know, the transformation from HCP phase to FCC phase occurs in several conditions including solidification [122,123], deformation [119,124], and heat treatment process. In essence, the formation of FCC phase is induced by mechanical stress or internal thermal stress [125,126]. And the forming mechanisms are related to the gliding of Shockley partial dislocations on every other {0001} planes in HCP matrix (Fig. 8) and pure-shuffle/shear-shuffle of atoms [127].

The lamellar FCC structures has been observed after the impact test by HUANG et al (Fig. 9(a)) [14]. From Fig. 9(b), it can be seen that the orientation relationship between FCC and α phases obeys: $\{0001\}_{\alpha}//\{111\}_{FCC}$ and $\langle 11\bar{2}0\rangle_{\alpha}//$

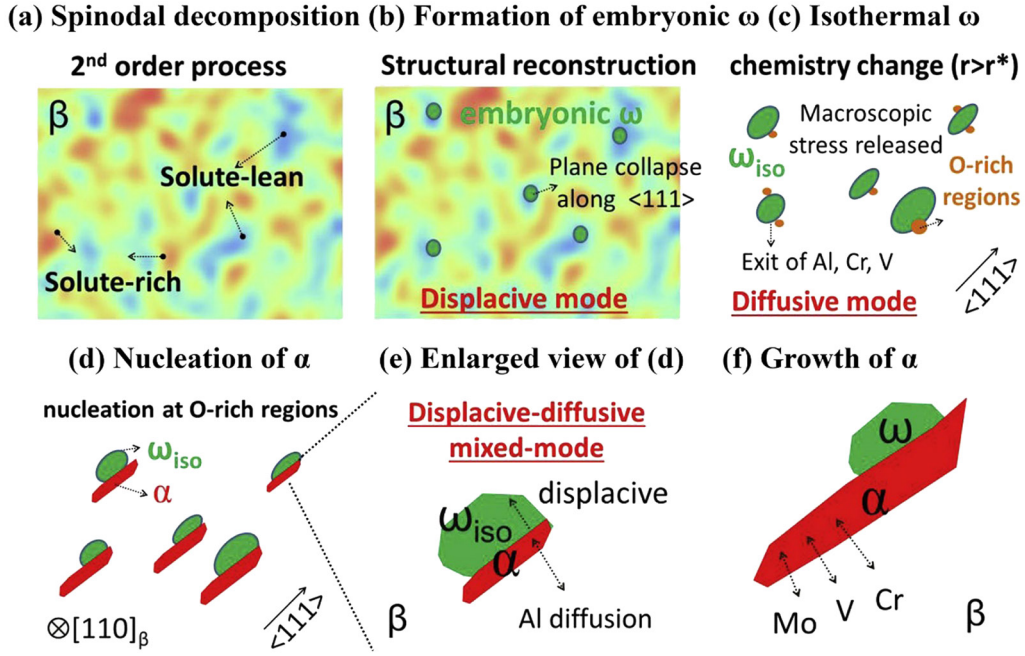

Fig. 7 Transformation pathways of embryonic ω to isothermal ω phase and then to α phase during isothermal aging (reproduced with permission from Ref. [98], Copyright (2016), Elsevier)

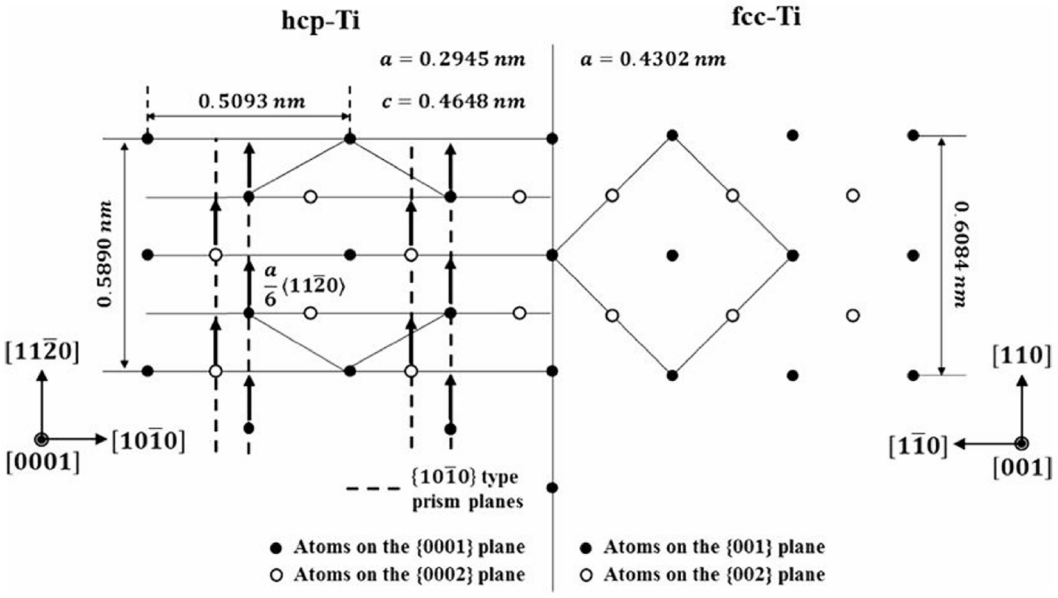

Fig. 8 Schematic diagram of transformation from HCP phase to FCC phase in pure Ti (reproduced with permission from Ref. [127], Copyright (2013), Elsevier)

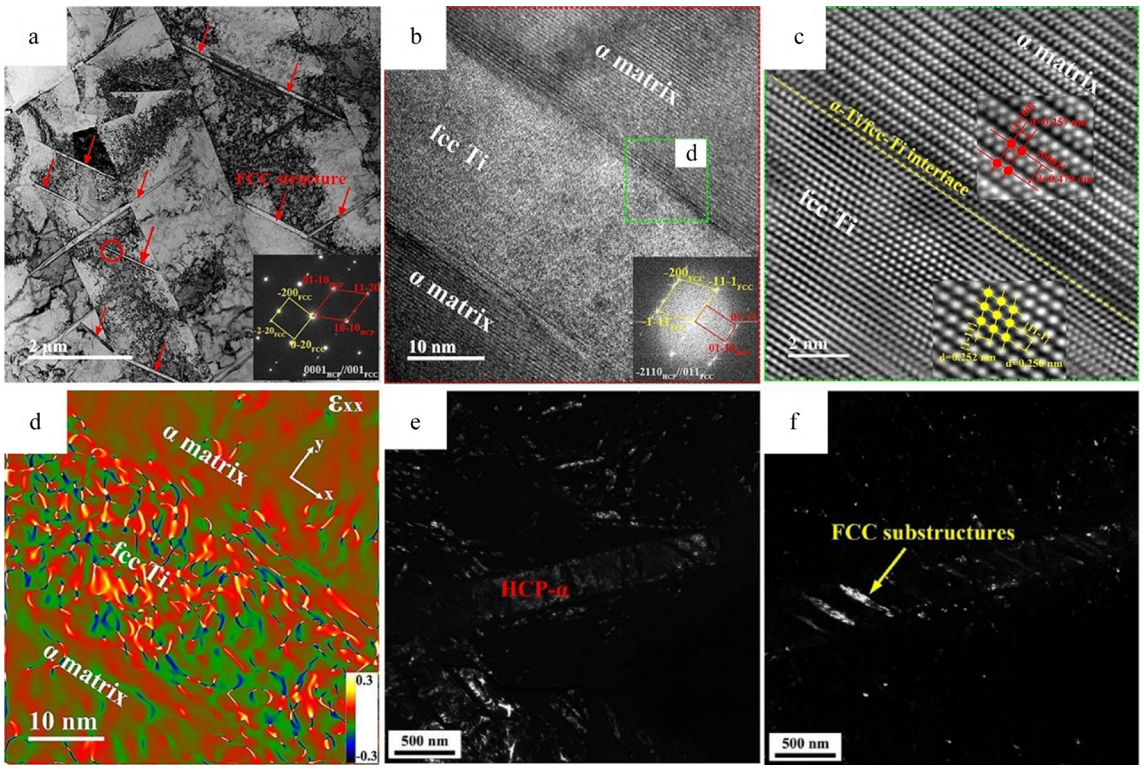

Fig. 9 TEM image of deformed titanium alloy showing presence of FCC structure (reproduced with permission from Ref. [14], Copyright (2024), Elsevier) (a); High-resolution TEM image and inserted FFT image of FCC phase and α matrix (reproduced with permission from Ref. [14], Copyright (2024), Elsevier) (b); Enlarged atomic image (c) of (b) and relative strain (ε_{xx}) map (d) of labeled region in (e) (reproduced with permission from Ref. [14], Copyright (2024), Elsevier); DF images of HCP α phase (e) and FCC substructures (f) in β titanium alloy (reproduced with permission from Ref. [13], Copyright (2022), Elsevier)

$\langle 1\bar{1}0\rangle_{FCC}$ with a coherent interface, as shown in Fig. 9(c). Besides, the corresponding geometrical phase analysis (GPA) image (Fig. 9(d)) has also been obtained, showing a severer strain distribution of FCC phase compared to the α matrix. This is considered to be related to the mismatch of lattice between the two phases [14]. Though FCC phase tends to be found in pure titanium and α-titanium alloys, it has also been observed in some β titanium alloys [13]. In these alloys, FCC phase is viewed as substructure in lamellar α phase, as shown in Figs. 9(e, f) [13].

It is worth noting that the α phase and FCC phase have two kinds of ORs in titanium alloys including basal plane type (B-type) and prismatic plane type (P-type) [119,120]. The former OR is in accordance with the OR shown in Fig. 9(b), while the latter one can be described as $\{10\bar{1}0\}_\alpha$// $\{110\}_{FCC}$ and $\langle 0001\rangle_\alpha$//$\langle 001\rangle_{FCC}$ [125]. Similar to other phases in titanium alloys, FCC phase also has various variants. According to the OR types of α phase and FCC phase, the features of FCC variants including the spatial morphology and crystallographic orientation distributions have been concluded by HU et al (as shown in Figs. 10(a, b)) [128]. It can be known that the two B-type FCC variants show a parallel relationship with each other (Fig. 10(a)) and the atomic structures are mirror-symmetric. However, for the P-type FCC phase, the three variants tend to display as 60°//$[001]_{FCC}$ relationship as shown in Fig. 10(b).

The FCC phase formation during HCP-$\alpha\rightarrow$ FCC transformation also has an indispensable effect on the mechanical properties of titanium alloys. It has been found by LI et al [121] that the existence of FCC structure has an obvious promoting effect on the improvement of ductility in a hot-rolled near-β titanium alloy. HUANG et al [14] pointed out that the transformation from α phase to FCC phase may have a similar effect on deformation twinning during the plastic deformation of α titanium alloys. This is mainly because of the shearing displacement caused by a pure-shuffle

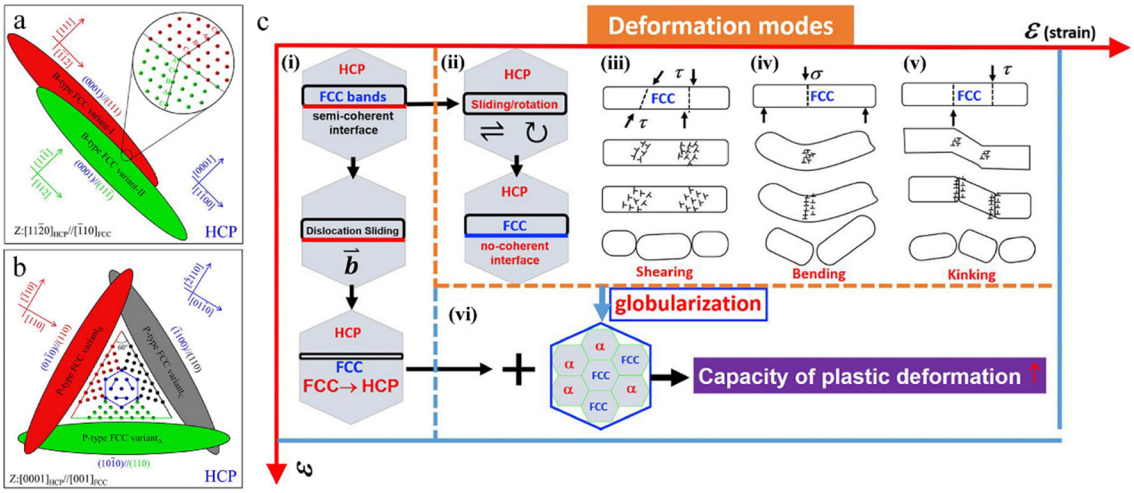

Fig. 10 Schematic diagram of B-type (a) and P-type (b) FCC variants (reproduced with permission from Ref. [128], Copyright (2023), Elsevier); Schematic diagram of deformation modes for FCC phase bands (reproduced with permission from Ref. [130], Copyright (2021), Elsevier) (c)

movement of several atomic layers [129] and more slip systems of FCC phase compared with the α matrix [130].

Besides, BAI et al [130] studied the deformation behavior of FCC bands during rolling process for high-purity titanium alloy. The results uncover two deformation paths with different modes under various rolling reductions, as shown in Fig. 10(c). One of the deformation paths can be seen in Stage (i), showing the FCC→HCP-α transformation activated by increasing the strain. Another deformation path is depicted as Stage (ii)−(v): (1) initially, the sliding and rotation of interphase boundary occurred, resulting in the non-coherent interface between HCP and FCC phases from semi-coherent interface; (2) with the increase in deformation strain, shearing, bending and kinking processes were observed to exist separately or compositely, resulting in the fragmentation and spheroidization of FCC bands. Finally, under the function of two deformation paths, the excellent capacity of plastic deformation can be achieved due to the combination effect of spheroidization and phase transformation as shown in Stage (vi) [130]. A strain partition was also found between lamellar FCC substructure and multi-scale distributed α phase by ZHU et al [131] together with excellent integrative properties including high tensile strength and ductility.

3.5 *O′* and *O″* phase transformation

It is well known that the formation of α' and α'' phases is a combination process of a partial shear and subsequent shuffle [2,132]. The interesting phenomenon is that when the order of shear and subsequent shuffle process is reversed, the phase transformation can be intermitted before the occurrence of shear process with the existence of an unusual metastable phase [133]. This metastable phase with orthorhombic lattice structure is called O' phase [16,133]. A series of researches have been conducted on the identification and formation of O' phase [16,134]. ZHENG et al [16] verified the presence of O' phase by the atomic scale characterization, as shown in Figs. 11(a−c). It can be seen that a $\{110\}\langle 1\bar{1}0\rangle$ shuffle occurred in β matrix, resulting in the formation of O' phase (Fig. 11(a)) with extra diffraction points (as shown in Figs. 11(b, c)). Some other reports show that when the concentration of some elements (e.g. Mo, Zr, and Al) reaches a certain value, O' phase can be induced and the formation process can be accelerated by the addition of O solute atom [134].

As a metastable phase, O' phase also plays an important role in the microstructural evolutions during transformation process and thus affects the mechanical properties of titanium alloys. For example, a continuous $\beta\rightarrow O'\rightarrow\alpha''$ transformation process has been found by LIANG et al [133], as shown in Figs. 11(d−g). Observations of the microstructure in a solutionized and quenched Ti2448 alloy were conducted to confirm the occurrence of $\beta\rightarrow O'$ transformation via a pure shuffle. Subsequently, the transformation from O'

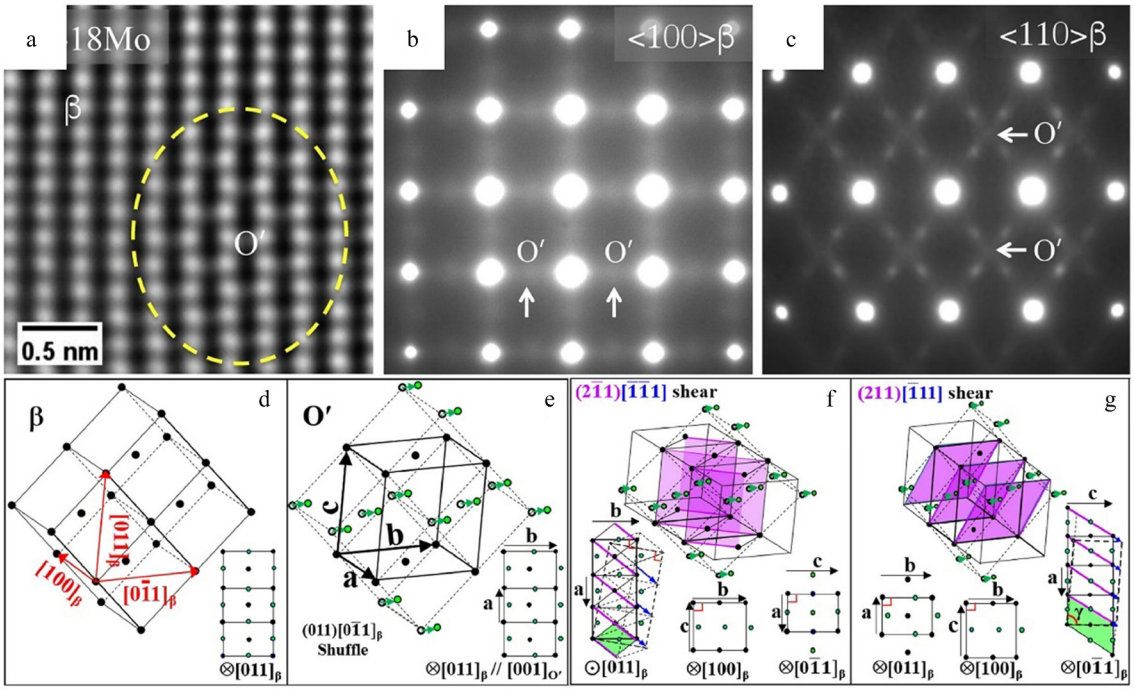

Fig. 11 Atomic structure of O' phase with $\{110\}\langle 1\bar{1}0\rangle$ shuffle in Ti−18Mo alloy (a), and SAED patterns along $\langle 100\rangle_\beta$ zone axis (b) and $\langle 110\rangle_\beta$ zone axis (c) (reproduced with permission from Ref. [16], Copyright (2016), Elsevier); Schematic diagrams showing β-phase structure (d), formation of O' phase from β phase (e), and $O'\rightarrow\alpha''$ transformation by $(2\bar{1}1)[\bar{1}\bar{1}1]$ shear (f) and $(211)[\bar{1}11]$ shear (g) (reproduced with permission from Ref. [133], Copyright (2020), Elsevier)

nanodomains to α'' nanodomains occurred with the increase of shear amount in O' phase during the cooling (below the room temperature) and loading processes [133]. And the $O'\rightarrow\alpha''$ transformation is considered to act as the essential mechanism bringing unique superelasticity of Ti-2448 alloy in a broad temperature range [133]. Nano-scaled O' phase has also been found to have the influence on the deformation behavior of a metastable β titanium alloy by affecting the formation types of the deformation twins [135].

With the exception of O' phase, O'' phase is also observed during the $\beta\rightarrow\alpha$ transformation. But different from O' phase, O'' phase is considered to be an ordered phase with orthorhombic lattice structure [18]. ZHENG et al [18] pointed out that the formation of O'' phase was a result of the ordering of every third $\{011\}_\beta$ plane promoted by Al segregation. And during the aging processes with gradually increasing the temperature, it was found that the presence of O' phase has a temperature range below 250 °C, while the formation of O'' phase was observed above 350 °C. The existence of temperature interval indicates that there is no transition from O' phase with shuffle-induced modulated structure to heating-induced O'' phase [18]. Apart from the temperature factor, the occurrence of O'' phase is also related to aging time [17]. The microstructure of a Ti-5553 alloy acquired by heating to 400 °C with a rate of 5 °C/min can be observed in Figs. 12(a, b). Except for the bright diffraction points of β and α phase, extra weak diffraction points of O'' phase can also be found with the help of intensity profile depicted by purple line in Fig. 12(e). However, when the aging time was increased to 15 h, the diffraction points of O'' phase disappeared, as shown in Figs. 12(c−e). The corresponding transition mechanism can be seen from Fig. 12(f), showing the assistant role of O'' phase helping the nucleation and growth of α phase [17].

4 Summary and prospect

In recent decades, due to excellent properties and broad application prospects, the researches on titanium alloys have acquired rapid development and remarkable achievements [136,137]. In order to

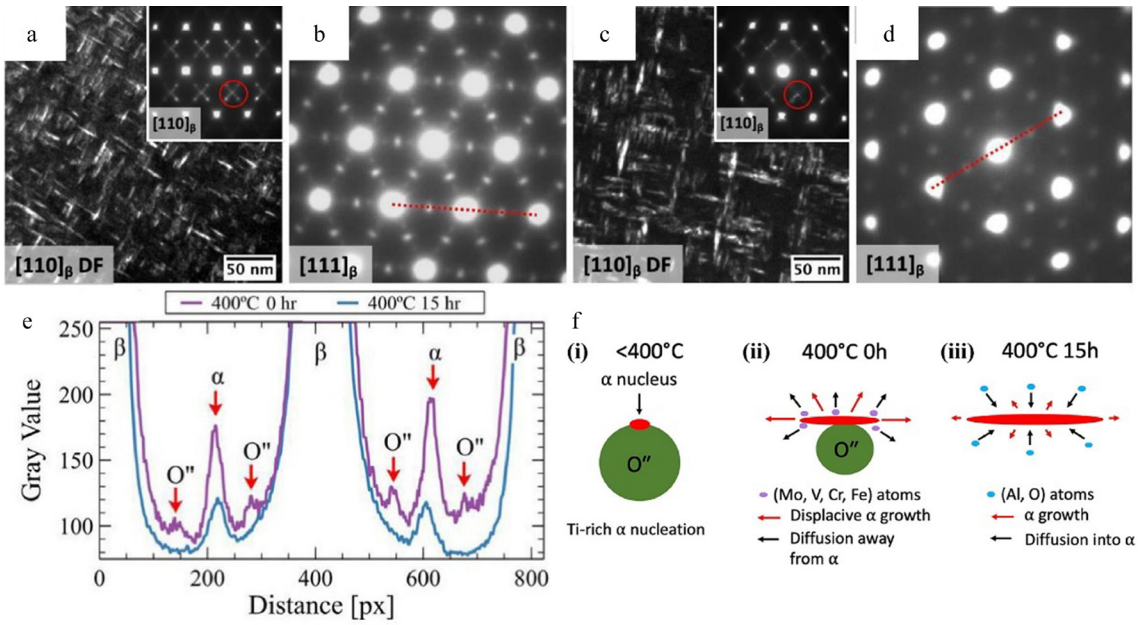

Fig. 12 DF-TEM images of *O″* phase obtained by heating treatment at 400 °C for 0 h (a) and 15 h (c) with SAED patterns along $[110]_\beta$ zone axis (b), and corresponding SAED patterns along $[111]_\beta$ zone axis (d); profiles (e) of gray-scale value intensity corresponding to red lines in (b) and (d); Schematic diagram showing nucleation and growth of α phase based on *O″* phase (f) (reproduced with permission from Ref. [17], Copyright (2021), Elsevier)

further expand their applications in a variety of fields, especially in extremely harsh environments, it is essential to achieve breakthroughs against the dilemma of strength−ductility trade-off. However, different from other alloy systems, there are various phases and phase transformations in titanium alloys, resulting in the extreme complexity of microstructure [138−140]. Therefore, a comprehensive and in-depth understanding of the phase transformation processes and their effects on the mechanical properties are vital important.

In this review, a series of phases including equilibrium phases (α and β phases) and metastable phases (β', α', α'', ω, FCC, O' and O'' phases) are discussed. It has been shown that phase transformation is a result of multiple factors, including internal composition and structural differences or externally applied mechanical/thermal stress, making atoms shuffle and shear to different degrees and thus obtaining a relative state among the $\beta\rightarrow\alpha$ transformation. As for the unstable state of metastable phases, titanium alloys with only equilibrium phases are generally preferred in engineering applications to ensure stable performance. On the other hand, metastable phases can act as the medium to assist the nucleation and growth of α phase. Thus, multi-scale α phase with different morphologies can be designed to achieve excellent properties on the basis of regulating the metastable phases. Besides, it is also helpful to widely and deeply understand the phase transformations for the failure analysis of titanium alloys applied to specific environment. It is worth noting that although various phases and correlated phase transformation have been widely studied, there are also a lot of unresolved issues for titanium alloys.

(1) How to controlling of phase transitions?

Affected by alloy composition, fabrication processing and heat treatment processes, various phase transitions in titanium alloys are difficult to control, and it is necessary to combine machine learning to establish a corresponding database to provide a reliable basis for the accurate control of phase transitions in titanium alloys. At the same time, further exploration of the phase transition mechanism is also required to realize the control of phase transition and revise the rules obtained by machine learning.

(2) How to utilize metastable phase?

Although there have been a lot of reports about various metastable phases formation during the $\beta\rightarrow\alpha$ transformation, in the actual production process, only two equilibrium phases are usually

used to regulate the mechanical properties of titanium alloys. On the basis of controlling the phase transitions, the metastable phase should be more efficiently utilized to improve the performance of titanium alloys.

(3) How to simplify preparation process?

In the actual fabrication process, in order to obtain excellent alloy properties, all kinds of complex fabrication process routes are adopted, but the current researches on the microstructural evolution of titanium alloy are only for simple alloy systems and preparation processes. Therefore, developing simple process routes and designing new high performance titanium alloy are very critical to achieve the improvement of alloy properties and also the controlling of the production cost.

CRediT authorship contribution statement

Chang-chang LIU: Writing − Original draft, Investigation, Formal analysis, Data curation; **Yang-huan-zi LI:** Investigation, Writing − Review & editing; **Ji GU:** Writing − Review & editing, Methodology, Formal analysis, Data curation, Conceptualization; **Min SONG:** Writing − Review & editing, Supervision, Project administration, Funding acquisition.

Declaration of competing interest

The authors declare that they have no known competing financial interests or personal relationships that could have appeared to influence the work reported in this paper.

Acknowledgments

This work was financially supported by the National Natural Science Foundation of China (Nos. U23A20540, 52371127), the Science and Technology Innovation Program of Hunan Province, China (No. 2022RC3035), and the Fundamental Research Funds for the Central Universities of Central South University, China (No. 2024ZZTS0077).

References

[1] ZHANG Hang, ZHANG Jin-yu, HOU Jing-peng, ZHANG Dong-dong, YUE Yong-hai, LIU Gang, SUN Jun. Making a low-cost duplex titanium alloy ultra-strong and ductile via interstitial solutes [J]. Acta Materialia, 2022, 241: 118411.

[2] ZHAO Qin-yang, SUN Qiao-yan, XIN She-wei, CHEN Yong-nan, WU Cong, WANG Huan, XU Jian-wei, WAN Ming-pan, ZENG Wei-dong, ZHAO Yong-qing. High-strength titanium alloys for aerospace engineering applications: A review on melting-forging process [J]. Materials Science and Engineering A, 2022, 845: 143260.

[3] XU Shuai, ZHANG Hai-ming, XIAO Na-min, QIU Ri-sheng, CUI Zhen-shan, FU Ming-wang. Mechanisms of macrozone elimination and grain refinement of near α Ti alloy via the spheroidization of the Widmannstätten structure [J]. Acta Materialia, 2023, 260: 119339.

[4] RAN Chun, SHENG Ze-min, CHEN Peng-wan, ZHANG Wang-feng, CHEN Qi. Effect of microstructure on the mechanical properties of Ti−5Al−5Mo−5V−1Cr−1Fe alloy [J]. Materials Science and Engineering A, 2020, 773: 138728.

[5] YANG J K, ZHANG C L, ZHANG H, LI J, ZHANG J Y, KUANG J, LIU G, SUN J. Spinodal decomposition-mediated multi-architectured α precipitates making a metastable β-Ti alloy ultra-strong and ductile [J]. Journal of Materials Science & Technology, 2024, 191: 106−121.

[6] XIAO Xiang, YANG Kun, LEI Shan, ZHANG De-chuang, GUO Lin, DAI Yi-long, LIN Jian-guo. A β-type titanium alloy with high strength and low elastic modulus achieved by spinodal decomposition [J]. Journal of Alloys and Compounds, 2023, 963: 171270.

[7] LI Diao-feng, BAI Chun-guang, ZHANG Zhi-qiang, WANG Ran, LI Nan, YANG Rui. α'' martensite engineering: A strategy to achieve high yield strength and low yield ratio synergy for dual-phase titanium alloy [J]. Materials & Design, 2024, 239: 112764.

[8] JIA Yan-di, MA Ying-jie, SU Hu-hu, HUANG Sen-sen, WANG Qian, QI Min, YANG Yu-jing, ZHENG Shi-jian, LEI Jia-feng, YANG Rui. The stress-induced α'' and its effect on the aging microstructure and mechanical properties in an $\alpha+\beta$ titanium alloy [J]. Materials Characterization, 2024, 209: 113734.

[9] DUMAS O, MALET L, HARY B, PRIMA F, GODET S. Crystallography and reorientation mechanism upon deformation in the martensite of an $\alpha-\alpha'$ Ti−6Al−4V dual-phase microstructure exhibiting high work-hardening rate [J]. Acta Materialia, 2021, 205: 116530.

[10] SANG Zhuo-yue, WANG Le, CHEN Jian-wei, FAN Qun-bo, ZHOU Sen, TAO Lei, WU Ya-yu, PENG Xiao-yang, ZHOU Zhi-ming, YAO Jia-hao. Excellent strength-ductility balance via controlling stress-induced α' martensite transformation of Ti422 alloy [J]. Materials Science and Engineering A, 2023, 884: 145558.

[11] NAG S, BANERJEE R, SRINIVASAN R, HWANG J Y, HARPER M, FRASER H L. ω-assisted nucleation and growth of α precipitates in the Ti−5Al−5Mo−5V−3Cr−0.5Fe β titanium alloy [J]. Acta Materialia, 2009, 57: 2136−2147.

[12] DEY G K, TEWARI R, BANERJEE S, JYOTI G, GUPTA S C, JOSHI K D, SIKKA S K. Formation of a shock deformation induced ω phase in Zr 20 Nb alloy [J]. Acta Materialia, 2004, 52: 5243−5254.

[13] LI X, WANG X N, LIU K, CAO G H, LI M B, ZHU Z S, WU S J. Hierarchical structure and deformation behavior of a novel multicomponent β titanium alloy with ultrahigh strength [J]. Journal of Materials Science & Technology,

2022, 107: 227−242.

[14] HUANG Shi-xing, YANG Zhong, ZHAO Qin-yang, ZHAO Yong-qing, LIN Cheng, YU Jia-shi, LI Jian-ping, ZHOU Ying-hui, YANG Xi-gang. Insights into multiple deformation mechanisms induced ultrahigh impact toughness of high-purity titanium [J]. Materials Characterization, 2024, 209: 113756.

[15] ZHOU Ya-chong, XU Xiao-feng, ZHAO Yang, YAN Xu-dong, WEI Lai, WU Zhi-cheng, WU Chao. Introducing ω and O' nanodomains in Ti−6Al−4V: The mechanism of accelerating $\alpha\rightarrow\beta$ transformation kinetics via electropulsing [J]. Journal of Materials Science & Technology, 2023, 162: 109−117.

[16] ZHENG Yu-feng, BANERJEE D, FRASER H L. A nano-scale instability in the β phase of dilute Ti−Mo alloys [J]. Scripta Materialia, 2016, 116: 131−134.

[17] ANTONOV S, SHI Rong-pei, LI Dian, KLOENNE Z, ZHENG Yu-feng, FRASER H L, RAABE D, GAULT B. Nucleation and growth of α phase in a metastable β-titanium Ti−5Al−5Mo−5V−3Cr alloy: Influence from the nano-scale, ordered-orthorhombic O'' phase and α compositional evolution [J]. Scripta Materialia, 2021, 194: 113672.

[18] ZHENG Yu-feng, ANTONOV S, FENG Qiang, BANERJEE R, BANERJEE D, FRASER H L. Shuffle-induced modulated structure and heating-induced ordering in the metastable β-titanium alloy, Ti−5Al−5Mo−5V−3Cr [J]. Scripta Materialia, 2020, 176: 7−11.

[19] PING D H, YAMABE-MITARAI Y, CUI C Y, YIN F X, CHOUDHRY M A. Stress-induced α'' martensitic (110) twinning in β-Ti alloys [J]. Applied Physics Letters, 2008, 93: 151911.

[20] AHMED M, WEXLER D, CASILLAS G, SAVVAKIN D G, PERELOMA E V. Strain rate dependence of deformation-induced transformation and twinning in a metastable titanium alloy [J]. Acta Materialia, 2016, 104: 190−200.

[21] ZHANG Chong-le, ZHANG Jin-yu, BAO Xiang-yun, LI Jiao, ZHANG Dong-dong, LIU Gang, SUN Jun. Hierarchically ordered coherent interfaces-driven ultrahigh specific-strength and toughness in a nano-martensite titanium alloy [J]. Acta Materialia, 2024, 263: 119540.

[22] GUAN X R, CHEN Q, QU S J, CAO G J, WANG H, RAN X D, FENG A H, CHEN D L. High-strain-rate deformation: Stress-induced phase transformation and nanostructures in a titanium alloy [J]. International Journal of Plasticity, 2023, 169: 103707.

[23] BRUMBAUER F, OKAMOTO N L, ICHITSUBO T, SPRENGEL W, LUCKABAUER M. Minor additions of Sn suppress the omega phase formation in beta titanium alloys [J]. Acta Materialia, 2024, 262: 119466.

[24] MATSUKAWA Y, OKUMA I, MUTA H, SHINOHARA Y, SUZUE R, YANG H L, MARUYAMA T, TOYAMA T, SHEN J J, LI Y F, SATOH Y, YAMANAKA S, ABE H. Crystallographic analysis on atomic-plane parallelisms between bcc precipitates and hcp matrix in recrystallized Zr−2.5Nb alloys [J]. Acta Materialia, 2017, 126: 86−101.

[25] FURUHARA T, OGAWA T, MAKI T. Atomic structure of interphase boundary of an a precipitate plate in a β Ti−Cr alloy [J]. Philosophical Magazine Letters, 2006, 72: 175−183.

[26] KITASHIMA T, HIROTO T, JODI D E, WATANABE M. Fabricating a single-crystal-like β grain structure of a near-β Ti alloy with unique variant selection by laser powder bed fusion [J]. Materials & Design, 2024, 243: 113039.

[27] GERMAIN L, GEY N, HUMBERT M, VO P, JAHAZI M, BOCHER P. Texture heterogeneities induced by subtransus processing of near α titanium alloys [J]. Acta Materialia, 2008, 56: 4298−4308.

[28] VAN BOHEMEN S M C, KAMP A, PETROV R H, KESTENS L A I, SIETSMA J. Nucleation and variant selection of secondary α plates in a β Ti alloy [J]. Acta Materialia, 2008, 56: 5907−5914.

[29] FURUHARA T, MAKI T. Variant selection in heterogeneous nucleation on defects in diffusional phase transformation and precipitation [J]. Materials Science and Engineering A, 2001, 312: 145−154.

[30] QIU D, SHI R, ZHANG D, LU W, WANG Y. Variant selection by dislocations during α precipitation in α/β titanium alloys [J]. Acta Materialia, 2015, 88: 218−231.

[31] BACHE M R, EVANS W J. Impact of texture on mechanical properties in an advanced titanium alloy [J]. Materials Science and Engineering A, 2001, 319/320/321: 409−414.

[32] EVANS W J, JONES J P, WHITTAKER M T. Texture effects under tension and torsion loading conditions in titanium alloys [J]. International Journal of Fatigue, 2005, 27: 1244−1250.

[33] BHATTACHARYYA D, VISWANATHAN G B, FRASER H L. Crystallographic and morphological relationships between β phase and the Widmanstätten and allotriomorphic α phase at special β grain boundaries in an α/β titanium alloy [J]. Acta Materialia, 2007, 55: 6765−6778.

[34] LIU Chang-chang, GU Ji, YI Jian-hong, LI Cai-ju, YAN Hong-ge, ZUBAIR M, SONG Min. Microstructures and mechanical properties of Ti-55511 alloy subjected to rolling in the $\alpha+\beta$ dual-phase region [J]. Intermetallics, 2024, 170: 108331.

[35] AN Xing-long, JIANG Wen-ting, NI Song, SONG Min. Effects of subtransus triplex heat treatments on the microstructure and mechanical behaviors of a Ti−5Al−5Mo−5V−1Cr−1Fe near β titanium alloy [J]. Materials Science and Engineering A, 2022, 859: 144207.

[36] RONG Wang, DUNLOP G L. The crystallography of secondary carbide precipitation in high speed steel [J]. Acta Metallurgica, 1984, 32: 1591−1599.

[37] ZHANG Ming-xing, KELLY P M. Crystallographic features of phase transformations in solids [J]. Progress in Materials Science, 2009, 54: 1101−1170.

[38] HE D, ZHU J C, ZAEFFERER S, RAABE D, LIU Y, LAI Z L, YANG X W. Influences of deformation strain, strain rate and cooling rate on the Burgers orientation relationship and variants morphology during $\beta\rightarrow\alpha$ phase transformation in a near α titanium alloy [J]. Materials Science and Engineering A, 2012, 549: 20−29.

[39] BANERJEE D, WILLIAMS J C. Perspectives on titanium science and technology [J]. Acta Materialia, 2013, 61: 844−879.

[40] ZHOU Yu, WANG Ke, LI Hong-hui, WEN Xin, XIN

Ren-long. Effect of content and configuration of equiaxed α and lamellar α on deformation mechanism and tensile properties of a near-α titanium alloy [J]. Materials Science and Engineering A, 2023, 877: 145192.

[41] SUN Shi-chen, FANG Hong-ze, LI Yi-li, CHEN Rui-run, ZHANG Xiao-fu, SU Yan-qing, GUO Jing-jie. Regulating phase ratio of β/α and static recrystallization of Ti−5Al−5Mo−5Cr−3Nb−2Zr with high plasticity alloyed by vanadium [J]. Materials Characterization, 2023, 203: 113090.

[42] DEVARAJ A, JOSHI V V, SRIVASTAVA A, MANANDHAR S, MOXSON V, DUZ V A, LAVENDER C. A low-cost hierarchical nanostructured beta-titanium alloy with high strength [J]. Nature Communications, 2016, 7: 11176.

[43] JIA C L, WU L H, XUE P, ZHANG H, NI D R, XIAO B L, MA Z Y. Static spheroidization and its effect on superplasticity of fine lamellae in nugget of a friction stir welded Ti−6Al−4V joint [J]. Journal of Materials Science & Technology, 2022, 119: 1−10.

[44] LIN Y C, XIAO Yi-wei, JIANG Yu-qiang, PANG Guo-dong, LI Hong-bin, ZHANG Xiao-yong, ZHOU Ke-chao. Spheroidization and dynamic recrystallization mechanisms of Ti-55511 alloy with bimodal microstructures during hot compression in $\alpha+\beta$ region [J]. Materials Science and Engineering A, 2020, 782: 139282.

[45] MA Rui, ZHANG Xin-fang. Eliminating the lamellar microstructure and improving the mechanical properties by optimizing the spheroidization of titanium alloys [J]. Materials Characterization, 2024, 212: 113950.

[46] DONG Xian-juan, LU Shi-qiang, ZHENG Hai-zhong. Dynamic spheroidization kinetics behavior of Ti−6.5Al−2Zr−1Mo−1V alloy with lamellar microstructure [J]. Transactions of Nonferrous Metals Society of China, 2016, 26: 1301−1309.

[47] GAO Peng-fei, FU Ming-wang, ZHAN Mei, LEI Zhen-ni, LI Yan-xi. Deformation behavior and microstructure evolution of titanium alloys with lamellar microstructure in hot working process: A review [J]. Journal of Materials Science & Technology, 2020, 39: 56−73.

[48] SESHACHARYULU T, MEDEIROS S C, MORGAN J T, MALAS J C, FRAZIER W G, PRASAD Y V R K. Hot deformation mechanisms in ELI Grade Ti−6A1−4V [J]. Scripta Materialia, 1999, 41: 283−288.

[49] BUZOLIN R H, LASNIK M, KRUMPHALS A, POLETTI M C. Hot deformation and dynamic α-globularization of a Ti-17 alloy: Consistent physical model [J]. Materials & Design, 2021, 197: 109266.

[50] LI L, LUO J, YAN J J, LI M Q. Dynamic globularization and restoration mechanism of Ti−5Al−2Sn−2Zr−4Mo−4Cr alloy during isothermal compression [J]. Journal of Alloys and Compounds, 2015, 622: 174−183.

[51] ZHEREBTSOV S, MURZINOVA M, SALISHCHEV G, SEMIATIN S L. Spheroidization of the lamellar microstructure in Ti−6Al−4V alloy during warm deformation and annealing [J]. Acta Materialia, 2011, 59: 4138−4150.

[52] SHARMA G, RAMANUJAN R V, TIWARI G P. Instability mechanisms in lamellar microstructures [J]. Acta Materialia, 2000, 48: 875−889.

[53] SEMIATIN S L, SEETHARAMAN V, WEISS I. Flow behavior and globularization kinetics during hot working of Ti−6Al−4V with a colony alpha microstructure [J]. Materials Science and Engineering A, 1999, 263: 257−271.

[54] WU Cheng-bao, YANG He, FAN Xiao-guang, SUN Zhi-chao. Dynamic globularization kinetics during hot working of TA15 titanium alloy with colony microstructure [J]. Transactions of Nonferrous Metals Society of China, 2011, 21: 1963−1969.

[55] ZHANG Jin-hu, JU Hong-tao, XU Hai-sheng, YANG Liang, MENG Zhi-chao, LIU Chen, SUN Ping, QIU Jian-ke, BAI Chun-guang, XU Dong-sheng, YANG Rui. Effects of heating rate on the alloy element partitioning and mechanical properties in equiaxed $\alpha+\beta$ Ti−6Al−4V alloy [J]. Journal of Materials Science & Technology, 2021, 94: 1−9.

[56] KOIKE J, SHIMOYAMA Y, OHNUMA I, OKAMURA T, KAINUMA R, ISHIDA K, MARUYAMA K. Stress-induced phase transformation during superplastic deformation in two-phase Ti−Al−Fe alloy [J]. Acta Materialia, 2000, 48: 2059−2069.

[57] LIU B, MATSUMOTO H, LI Y P, KOIZUMI Y, LIU Y, CHIBA A. Dynamic phase transformation during hot-forging process of a powder metallurgy $\alpha+\beta$ titanium alloy [J]. Materials Transactions, 2012, 53: 1007−1010.

[58] DING Ran, YAO Ying-jie, SUN Bin-han, LIU Geng, HE Jian-guo, LI Tong, WAN Xin-hao, DAI Zong-biao, PONGE D, RAABE D, ZHANG C, GODFREY A, MIYAMOTO G, FURUHARA T, YANG Zhi-gang, ZWAAG S V D, HAO Che. Chemical boundary engineering: A new route toward lean, ultrastrong yet ductile steels [J]. Science Advances, 2020, 6: 1430.

[59] XIN Tong-zheng , ZHAO Yu-hong , MAHJOUB R, JIANG Jia-xi, YADAV A, KEITA N. Ultrahigh specific strength in a magnesium alloy strengthened by spinodal decomposition [J]. Science Advances, 2021, 7: 3039.

[60] XIAO Wen-long, DARGUSCH M S, KENT D, ZHAO Xin-qing, MA Chao-li. Activation of homogeneous precursors for formation of uniform and refined α precipitates in a high-strength β-Ti alloy [J]. Materialia, 2020, 9: 100557.

[61] BARRIOBERO-VILA P, REQUENA G, SCHWARZ S, WARCHOMICKA F, BUSLAPS T. Influence of phase transformation kinetics on the formation of α in a β-quenched Ti−5Al−5Mo−5V−3Cr−1Zr alloy [J]. Acta Materialia, 2015, 95: 90−101.

[62] AFONSO C R M, FERRANDINI P L, RAMIREZ A J, CARAM R. High resolution transmission electron microscopy study of the hardening mechanism through phase separation in a β-Ti−35Nb−7Zr−5Ta alloy for implant applications [J]. Acta Biomaterialia, 2010, 6: 1625−1629.

[63] AN Zi-bing, MAO Sheng-cheng, YANG Tao, LIU C T, ZHANG Bin, MA E, ZHOU Hao, ZHANG Ze, WANG Li-hua, HAN Xiao-dong. Spinodal-modulated solid solution delivers a strong and ductile refractory high-entropy alloy [J]. Materials Horizons, 2021, 8: 948−955.

[64] SENKOV O N, JENSEN J K, PILCHAK A L, MIRACLE D B, FRASER H L. Compositional variation effects on the microstructure and properties of a refractory high-entropy

superalloy AlMo0.5NbTa0.5TiZr [J]. Materials & Design, 2018, 139: 498−511.

[65] GEORGE A, DIVAKAR R. Evidence for spinodal decomposition in Ti−15Mo quenched alloy using transmission electron microscopy [J]. Micron, 2019, 121: 43−52.

[66] ZHU Y M, ZHU S M, DARGUSCH M S, NIE J F. HAADF-STEM study of phase separation and the subsequent α phase precipitation in a β-Ti alloy [J]. Scripta Materialia, 2016, 112: 46−49.

[67] DEVARAJ A, NAG S, SRINIVASAN R, WILLIAMS R E A, BANERJEE S, BANERJEE R, FRASER H L. Experimental evidence of concurrent compositional and structural instabilities leading to ω precipitation in titanium−molybdenum alloys [J]. Acta Materialia, 2012, 60: 596−609.

[68] ZHENG Yu-feng, WILLIAMS R E A, WANG Dong, SHI Rong-pei, NAG S, KAMI P, SOSA J M, BANERJEE R, WANG Yun-zhi, FRASER H L. Role of ω phase in the formation of extremely refined intragranular α precipitates in metastable β-titanium alloys [J]. Acta Materialia, 2016, 103: 850−858.

[69] KATO M. Hardening by spinodally modulated structure in b.c.c. alloys [J]. Acta Metallurgica, 1981, 29: 79−87.

[70] CHEN Wei, YU Guo-xiang, LI Ke-er, WANG Yue, ZHANG Jin-yu, SUN Jun. Plastic instability in Ti−6Cr−5Mo−5V−4Al metastable β-Ti alloy containing the β-spinodal decomposition structures [J]. Materials Science and Engineering A, 2021, 811: 141052.

[71] BASU I, OCELíK V, DE H J T M. Size dependent plasticity and damage response in multiphase body centered cubic high entropy alloys [J]. Acta Materialia, 2018, 150: 104−116.

[72] NITOL M S, DICKEL D E, BARRETT C D. Machine learning models for predictive materials science from fundamental physics: An application to titanium and zirconium [J]. Acta Materialia, 2022, 224: 117347.

[73] NIINOMI M, KOBAYASHI T, INAGAKI I, THOMPSON A W. The effect of deformation-induced transformation on the fracture toughness of commercial titanium alloys [J]. Metallurgical Transactions A, 1990, 21: 1733−1744.

[74] BHATTACHARJEE A, VARMA V K, KAMAT S V, GOGIA A K, BHARGAVA S. Influence of β grain size on tensile behavior and ductile fracture toughness of titanium alloy Ti−10V−2Fe−3Al [J]. Metallurgical and Materials Transactions A−Physical Metallurgy and Materials Science, 2006, 37: 1423−1433.

[75] AHMED T, RACK H J. Phase transformations during cooling in α+β titanium alloys [J]. Materials Science and Engineering A, 1998, 243: 206−211.

[76] LEE H J, KIM J H, PARK C H, HONG J K, YEOM J T, LEE T, LEE S W. Twinning-induced plasticity mechanism of α''-martensitic titanium alloy [J]. Acta Materialia, 2023, 248: 118763.

[77] TAHARA M, KANAYA T, KIM H Y, INAMURA T, HOSODA H, MIYAZAKI S. Heating-induced martensitic transformation and time-dependent shape memory behavior of Ti−Nb−O alloy [J]. Acta Materialia, 2014, 80: 317−326.

[78] XU W, KIM K B, DAS J, CALIN M, ECKERT J. Phase stability and its effect on the deformation behavior of Ti−Nb−Ta−In/Cr β alloys [J]. Scripta Materialia, 2006, 54: 1943−1948.

[79] KIM H Y, SATORU H, KIM J I, HOSODA H, MIYAZAKI S. Mechanical properties and shape memory behavior of Ti−Nb alloys [J]. Materials Transactions, 2004, 45: 2443−2448.

[80] BHATTACHARJEE A, BHARGAVA S, VARMA V K, KAMAT S V, GOGIA A K. Effect of β grain size on stress induced martensitic transformation in β solution treated Ti−10V−2Fe−3Al alloy [J]. Scripta Materialia, 2005, 53: 195−200.

[81] PARADKAR A, KAMAT S V, GOGIA A K, KASHYAP B P. Trigger stress for stress-induced martensitic transformation during tensile deformation in Ti−Al−Nb alloys: Effect of grain size [J]. Metallurgical and Materials Transactions A−Physical Metallurgy and Materials Science, 2008, 39: 551−558.

[82] SUN F, ZHANG J Y, VERMAUT P, CHOUDHURI D, ALAM T, MANTRI S A, SVEC P, GLORIANT T, JACQUES P J, BANERJEE R, PRIMA F. Strengthening strategy for a ductile metastable β-titanium alloy using low-temperature aging [J]. Materials Research Letters, 2017, 5: 547−553.

[83] LEE S W, OH J M, KIM J H, PARK C H, HONG J K, YEOM J T. Demonstration of martensite reorientation-induced plasticity by ultra-high strength titanium alloys [J]. Materials Science and Engineering A, 2021, 807: 140878.

[84] LI C, WU X, CHEN J H, VAN D Z S. Influence of α morphology and volume fraction on the stress-induced martensitic transformation in Ti−10V−2Fe−3Al [J]. Materials Science and Engineering A, 2011, 528: 5854−5860.

[85] ZHENG Xiao-dong, ZHENG Shi-jian, WANG Jian, MA Ying-jie, WANG Hao, ZHOU Yang-tao, SHAO Xiao-hong, ZHANG Bo, LEI Jia-feng, YANG Rui, MA Xiu-liang. Twinning and sequential kinking in lamellar Ti−6Al−4V alloy [J]. Acta Materialia, 2019, 181: 479−490.

[86] AEBY-GAUTIER E, SETTEFRATI A, BRUNESEAUX F, APPOLAIRE B, DENAND B, DEHMAS M, GEANDIER G, BOULET P. Isothermal α'' formation in β metastable titanium alloys [J]. Journal of Alloys and Compounds, 2013, 577: 439−443.

[87] BARRIOBERO-VILA P, BIANCARDI OLIVEIRA V, SCHWARZ S, BUSLAPS T, REQUENA G. Tracking the α'' martensite decomposition during continuous heating of a Ti−6Al−6V−2Sn alloy [J]. Acta Materialia, 2017, 135: 132−143.

[88] TAHARA M, HASUNUMA K, IBAKI R, INAMURA T, HOSODA H. Microstructural evolution in β-metastable Ti−Mo−Sn−Al alloy during isothermal aging [J]. Advanced Engineering Materials, 2019, 21: 1900416.

[89] REN X B, WANG Y, ZHOU Y M, ZHANG Z, WANG D, FAN G L, OTSUKA K, SUZUKI T, JI Y C, ZHANG J, TIAN Y, HOU S, DING X D. Strain glass in ferroelastic systems: Premartensitic tweed versus strain glass [J]. Philosophical Magazine, 2010, 90: 141−157.

[90] BÖNISCH M, STOICA M, CALIN M. Routes to control diffusive pathways and thermal expansion in Ti-alloys [J]. Scientific Reports, 2020, 10: 3045.

[91] QI Lu, HE Su-yun, CHEN Chun-jin, JIANG Bin-bin, HAO Yu-lin, YE Heng-qiang, YANG Rui, DU Kui. Diffusional-

displacive transformation in a metastable β titanium alloy and its strengthening effect [J]. Acta Materialia, 2020, 195: 151−162.

[92] HE Bei, CHENG Xu, LI Jia, LI Guo-Chao, WANG Hua-ming. ω-assisted α phase and hardness of Ti−5Al−5Mo−5V−1Cr−1Fe during low temperature isothermal heat treatment after laser surface remelting [J]. Journal of Alloys and Compounds, 2017, 708: 1054−1062.

[93] CHOU K, LI N, MARQUIS E A. Enhanced work hardening from oxygen-stabilized ω precipitates in an aged metastable β Ti−Nb alloy [J]. Acta Materialia, 2021, 220: 117302.

[94] CHOUDHURI D, ZHENG Y, ALAM T, SHI R, HENDRICKSON M, BANERJEE S, WANG Y, SRINIVASAN S G, FRASER H, BANERJEE R. Coupled experimental and computational investigation of omega phase evolution in a high misfit titanium-vanadium alloy [J]. Acta Materialia, 2017, 130: 215−228.

[95] FONTAINE D. Mechanical instabilities in the b.c.c. lattice and the beta to omega phase transformation [J]. Acta Metallurgica, 1970, 18: 275−279.

[96] MANTRI S A, DASARI S, SHARMA A, ZHENG Y, FRASER H L, BANERJEE R. Role of aluminum rejection from isothermal ω precipitates on the formation of α precipitates in the metastable β-titanium alloy Ti−10V−2Fe−3Al [J]. Scripta Materialia, 2023, 234: 115565.

[97] CHEN Wei, CAO Shuo, KOU Wen-juan, ZHANG Jin-yu, WANG Yue, ZHA You, PAN Yan, HU Qing-miao, SUN Qiao-yan, SUN Jun. Origin of the ductile-to-brittle transition of metastable β-titanium alloys: Self-hardening of ω-precipitates [J]. Acta Materialia, 2019, 170: 187−204.

[98] LI Tong, KENT D, SHA Gang, STEPHENSON L T, CEGUERRA A V, RINGER S P, DARGUSCH M S, CAIRNEY J M. New insights into the phase transformations to isothermal ω and ω-assisted α in near β-Ti alloys [J]. Acta Materialia, 2016, 106: 353−366.

[99] WILLIAMS J C, HICKMAN B S, MARCUS H L. The effect of omega phase on the mechanical properties of titanium alloys [J]. Metallurgical Transactions, 1971, 2: 1913−1919.

[100] BOWEN A W. Omega phase embrittlement in aged Ti−15%Mo [J]. Scripta Metallurgica, 1971, 5: 709−715.

[101] WANG X L, LI L, MEI W, WANG W L, SUN J. Dependence of stress-induced omega transition and mechanical twinning on phase stability in metastable β Ti−V alloys [J]. Materials Characterization, 2015, 107: 149−155.

[102] WANG X L, LI L, XING H, OU P, SUN J. Role of oxygen in stress-induced ω phase transformation and $\{332\}\langle 113\rangle$ mechanical twinning in β Ti−20V alloy [J]. Scripta Materialia, 2015, 96: 37−40.

[103] WU S Q, PING D H, YAMABE-MITARAI Y, XIAO W L, YANG Y, HU Q M, LI G P, YANG R. $\{112\}\langle 111\rangle$ Twinning during ω to body-centered cubic transition [J]. Acta Materialia, 2014, 62: 122−128.

[104] LI L, MEI W, XING H, WANG X L, SUN J. Zigzag configuration of mechanical twin and stress-induced omega phase in metastable β Ti−34Nb (at.%) alloy [J]. Journal of Alloys and Compounds, 2015, 625: 188−192.

[105] SUN F, ZHANG J Y, MARTELEUR M, GLORIANT T, VERMAUT P, LAILLÉ D, CASTANY P, CURFS C, JACQUES P J, PRIMA F. Investigation of early stage deformation mechanisms in a metastable β titanium alloy showing combined twinning-induced plasticity and transformation-induced plasticity effects [J]. Acta Materialia, 2013, 61: 6406−6417.

[106] HIDA M, SUKEDAI E, TERAUCHI H. Microscopic approaches to isothermal transformation of incommensurate omega phase zones in Ti−20wt.%Mo alloy studied by XDS, HREM and EXAFS [J]. Acta Metallurgica, 1988, 36: 1429−1441.

[107] JONES N G, DASHWOOD R J, JACKSON M, DYE D. β phase decomposition in Ti−5Al−5Mo−5V−3Cr [J]. Acta Materialia, 2009, 57: 3830−3839.

[108] DUERIG T W, TERLINDE G T, WILLIAMS J C. Phase transformations and tensile properties of Ti−10V−2Fe−3Al [J]. Metallurgical Transactions A, 1980, 11: 1987−1998.

[109] LAI M J, LI T, YAN F K, LI J S, RAABE D. Revisiting ω phase embrittlement in metastable β titanium alloys: Role of elemental partitioning [J]. Scripta Materialia, 2021, 193: 38−42.

[110] TANE M, NISHIO H, EGUSA D, SASAKI T T, ABE E, MIYOSHI E, HIGASHINO S. Effects of aluminum and oxygen additions on quenched-in compositional fluctuations, dynamic atomic shuffling, and their resultant diffusionless isothermal ω transformation in ternary Ti−V-based alloys with bcc structure [J]. Acta Materialia, 2023, 255: 119034.

[111] GYSLER A, LÜTJERING G, GEROLD V. Deformation behavior of age-hardened Ti−Mo alloys [J]. Acta Metallurgica, 1974, 22: 901−909.

[112] LEVINE E, HAYDEN S Z, MARGOLIN H. Deformation behavior of an omega hardened alpha-beta titanium alloy [J]. Acta Metallurgica, 1974, 22: 1443−1448.

[113] TANE M, NISHIYAMA H, UMEDA A, OKAMOTO N L, INOUE K, LUCKABAUER M, NAGAI Y, SEKINO T, NAKANO T, ICHITSUBO T. Diffusionless isothermal omega transformation in titanium alloys driven by quenched-in compositional fluctuations [J]. Physical Review Materials, 2019, 3: 043604.

[114] OKAMOTO N L, KASATANI S, LUCKABAUER M, ENZINGER R, TSUTSUI S, TANE M, ICHITSUBO T. Evolution of microstructure and variations in mechanical properties accompanied with diffusionless isothermal ω transformation in β-titanium alloys [J]. Physical Review Materials, 2020, 4: 123603.

[115] ZHENG Y F, WILLIAMS R E A, SOSA J M, WANG Y Z, BANERJEE R, FRASER H L. The role of the ω phase on the non-classical precipitation of the α phase in metastable β-titanium alloys [J]. Scripta Materialia, 2016, 111: 81−84.

[116] ZHENG Y F, WILLIAMS R E A, SOSA J M, ALAM T, WANG Y Z, BANERJEE R, FRASER H L. The indirect influence of the ω phase on the degree of refinement of distributions of the α phase in metastable β-titanium alloys [J]. Acta Materialia, 2016, 103: 165−173.

[117] ZHANG Feng, FENG Jun, XIANG Wei, FU Qiang, YUAN Wu-hua. Enhanced mechanical properties in metastable β titanium alloy via ω-assisted nucleation [J]. Materials Science and Engineering A, 2022, 858: 144082.

[118] MANTRI S A, CHOUDHURI D, ALAM T, VISWANATHAN G B, SOSA J M, FRASER H L,

BANERJEE R. Tuning the scale of α precipitates in β-titanium alloys for achieving high strength [J]. Scripta Materialia, 2018, 154: 139−144.

[119] WEI Bing-qiang, NI Song, LIU Yong, LIAO Xiao-zhou, SONG Min. Phase transformation and structural evolution in a Ti−5at.%Al alloy induced by cold-rolling [J]. Journal of Materials Science & Technology, 2020, 49: 211−223.

[120] ZHENG Xiao-dong, GONG Ming-yu, XIONG Ting, GE Hua-long, YANG Li-xin, ZHOU Yang-tao, ZHENG Shi-jian, WANG Jian, MA Xiu-liang. Deformation induced FCC lamellae and their interaction in commercial pure Ti [J]. Scripta Materialia, 2019, 162: 326−330.

[121] LI Yang-huanzi, NI Song, LIU Yong, SONG Min. Phase transition induced high strength and large ductility of a hot rolled near β Ti−5Al−5Mo−5V−1Cr−1Fe alloy [J]. Scripta Materialia, 2019, 170: 34−37.

[122] YUAN Fu-sen, HAN Fu-zhou, ZHANG Ying-dong, MUHAMMAD Ali, GUO Wen-bin, REN Jie, LIU Cheng-ze, GU Heng-fei, LI Ge-ping, YUAN Gai-huan. Intermediate state of hexagonal close-packed structure to face-centered cubic structure transformation: Direct evidence for basal-type face-centered cubic phase via partial dislocation in zirconium [J]. Journal of Materials Science & Technology, 2022, 98: 44−50.

[123] LIU Cheng-ze, LI Ge-ping, GU Heng-fei, YUAN Fu-sen, HAN Fu-zhou, ALI M, ZHANG Ying-dong, GUO Wen-bin. Observation of FCC-Zr phase in as-cast Zircaloy-4 alloy [J]. Materials Letters, 2020, 267: 127551.

[124] ZHAO Heng-lv, SONG Min, NI Song, SHAO Shuai, WANG Jian, LIAO Xiao-zhou. Atomic-scale understanding of stress-induced phase transformation in cold-rolled Hf [J]. Acta Materialia, 2017, 131: 271−279.

[125] YUAN Fu-sen, LI Ge-ping, HAN Fu-zhou, ZHANG Ying-dong, MUHAMMAD A, GUO Wen-bin, REN Jie, LIU Cheng-ze, GU Heng-fei, YUAN Gai-huan. A new type face-centered cubic zirconium phase in pure zirconium [J]. Journal of Materials Science & Technology, 2021, 81: 236−239.

[126] YUAN F S, LI G P, HAN F Z, ZHANG Y D, MUHAMMAD A, GUO W B, REN J, LIU C Z, GU H F. New insight into prismatic-type face-centered cubic zirconium phase in pure zirconium [J]. Journal of Materials Science, 2021, 56: 2631−2637.

[127] HONG D H, LEE T W, LIM S H, KIM W Y, HWANG S K. Stress-induced hexagonal close-packed to face-centered cubic phase transformation in commercial-purity titanium under cryogenic plane-strain compression [J]. Scripta Materialia, 2013, 69: 405−408.

[128] HU Jia-nan, ZHANG Ying-dong, HAN Fu-zhou, GUO Wen-bin, ALI M, REN Jie, WANG Qi-chen, LI Ge-ping. Variants of face-centered cubic phase in pure hafnium during the HCP→FCC phase transformation [J]. Materials Characterization, 2023, 206: 113451.

[129] WU H C, KUMAR A, WANG J, BI X F, TOMÉ C N, ZHANG Z, MAO S X. Rolling-induced face centered cubic titanium in hexagonal close packed titanium at room temperature [J]. Scientific Reports, 2016, 6: 24370.

[130] BAI Feng-mei, YIN Li-bo, ZHAO Wei, ZHOU Hong-wei, SONG Meng, LIU Yan-chun, LIU Xiang-hua. Deformational behavior of face-centered cubic (FCC) phase in high-pure titanium [J]. Materials Science and Engineering A, 2021, 800: 140287.

[131] ZHU W G, KOU W J, TAN C S, ZHANG B Y, CHEN W, SUN Q Y, XIAO L, SUN J. Face centered cubic substructure and improved tensile property in a novel β titanium alloy Ti−5Al−4Zr−10Mo−3Cr [J]. Materials Science and Engineering A, 2020, 771: 138611.

[132] YUMAK N, ASLANTAŞ K. A review on heat treatment efficiency in metastable β titanium alloys: The role of treatment process and parameters [J]. Journal of Materials Research and Technology, 2020, 9: 15360−15380.

[133] LIANG Qiang-long, WANG Dong, ZHENG Yu-feng, ZHAO Shuang-shuang, GAO Yi-peng, HAO Yu-lin, YANG Rui, BANERJEE D, FRASER H L, WANG Yun-zhi. Shuffle-nanodomain regulated strain glass transition in Ti−24Nb−4Zr−8Sn alloy [J]. Acta Materialia, 2020, 186: 415−424.

[134] ZHENG Y F, ALAM T, BANERJEE R, BANERJEE D, FRASER H L. The influence of aluminum and oxygen additions on intrinsic structural instabilities in titanium−molybdenum alloys [J]. Scripta Materialia, 2018, 152: 150−153.

[135] LIANG Q L, KLOENNE Z, ZHENG Y F, WANG D, ANTONOV S, GAO Y P, HAO Y L, YANG R, WANG Y Z, FRASER H L. The role of nano-scaled structural non-uniformities on deformation twinning and stress-induced transformation in a cold rolled multifunctional β-titanium alloy [J]. Scripta Materialia, 2020, 177: 181−185.

[136] PENG Shu-xian, LIU Yi-kui, FU Ming-zhu, LIANG Yuan-long, ZHANG Kai, FENG Chun, FENG Wei-zhong, ZHANG Ping-hui, LIU Hui-qun. Synergistically achieving high strength and impact toughness in Ti−6Al−4V−0.5Mo−0.5Zr alloy pipe with bimodal microstructure [J]. Materials Science and Engineering A, 2024, 895: 146217.

[137] WU Gui-cheng, LI Si-yun, LI Jia-hui, CHEN Jing, LI Rui, GUO Jin-bang, WANG Xiao-xiang, WANG Ding-chun, CHEN Zhan-qian, LIN Yong-cheng, LIU Hui-qun. Texture evolution during multi-pass cold rolling and annealing of Ti−2Al−1.5Mn alloy [J]. Journal of Alloys and Compounds, 2024, 971: 172705.

[138] HU Xin, QI Lin, LIU Chao-qiang, CHEN Hou-wen, ZHANG Xiao-yong, YAN Hong-ge, ZHOU Ke-chao, SONG Min. Formation mechanism of stacking faults within α'' martensite in Ti−7wt.%Mo alloy [J]. Journal of Alloys and Compounds, 2023, 934: 168039.

[139] MA Sheng-nan, HU Xin, LIU Chao-qiang, QIU Shi-jia, SONG Min. Evolutions of the microstructures and mechanical properties of Ti−2.8wt.%Cu alloy during heat treatment [J]. Journal of Alloys and Compounds, 2024, 970: 172568.

[140] LIU Chao-qiang, XIE Zong-yu, ZHANG Xiao-yong, YAN Hong-ge, ZHOU Ke-chao, SONG Min. Mechanical properties and deformation behaviors of Ti−5Al−5Mo−1Fe−1Cr alloy with duplex and single-phase microstructures [J]. Transactions of Nonferrous Metals Society of China, 2023, 33: 1425−1436.

钛合金相变综述

刘畅畅，李杨欢子，顾 及，宋 旼

中南大学 粉末冶金国家重点实验室，长沙 410083

摘 要：近年来，钛及钛合金由于具有一系列优异的性能受到了广泛的关注。与其他合金体系不同，钛合金中存在着两种同素异形体和一系列亚稳相。在总结近年来研究成果的基础上，综述了钛合金中存在的各种相变过程，其中不仅涉及到了一些常见的相，还有部分较少被报道的相。对于钛合金中只涉及 α 相和 β 相的相变，不仅介绍了从 β 到 α 相的转变过程，还对其逆相变进行了描述，并阐述了应力在其中发挥的作用。对于亚稳相，从亚稳相的形成机理、其形成对微观结构和合金力学性能的影响等方面分别进行了论述。此外，还针对目前钛合金在发展过程中存在的问题提出了几点意见和建议。

关键词：钛合金；相变；显微组织演变；力学性能

(Edited by Bing YANG)